Chem Soc Rev

The reactivity of the active metal oxo and hydroxo intermediates and its implications in oxidations

Journal:	*Chemical Society Reviews*
Manuscript ID:	CS-TRV-07-2014-000244.R2
Article Type:	Tutorial Review
Date Submitted by the Author:	17-Jul-2014
Complete List of Authors:	Yin, Guochuan; Huazhong University of Science and Technology, School of Chemistry and Chemical Engineering Chen, Zhuqi; Huazhong University of Science and Technology,

Journal Name

RSCPublishing

ARTICLE

The reactivity of the active metal oxo and hydroxo intermediates and its implications in oxidations

Cite this: DOI: 10.1039/x0xx00000x

Zhuqi Chen and Guochuan Yin*

Received 00th January 2012,
Accepted 00th January 2012

DOI: 10.1039/x0xx00000x

www.rsc.org/

While the significance of the redox metal oxo moieties have been fully acknowledged in versatile oxidation processes, active metal hydroxo moieties are gradually realized to play the key roles in certain biological oxidation events, and their reactivity has also been evidenced by related biomimic models. However, compared with the metal oxo moieties, the significance of the metal hydroxo moieties has not been fully recognized, and their relationships in oxidations remains elusive until recently. This review summarizes the reactivity of the metal oxo and hydroxo moieties in different oxidation processes including hydrogen atom transfer, oxygen atom transfer and electron transfer, and their reactivity similarities and differences have been discussed as well. Particularly, how the physicochemical properties like metal-oxygen bond order, net charge and potential of a redox metal ion affect its reactivity has also been presented based on available data. We hope this review may provide new clues to understand the origins of the enzyme's choice on them in a specific event, to explain the elusive phenomena occurring in those enzymatic, homogeneous and heterogeneous oxidations, to design selective redox catalysts and control their reactivity.

Key Learning Points

1) The knowledge about the reactivity of the active metal oxo moieties in oxidations.
2) The knowledge about the reactivity of the active metal hydroxo moieties in oxidations.
3) The reactivity similarities and differences of the active metal oxo and hydroxo moieties in oxidations.
4) The trends of the reactivity change of a redox metal ion with its physicochemical properties.
5) The implications of the relationships between active metal oxo and hydroxo moieties in oxidations.

1 Introduction

Transition metal ions play the crucial roles in a series of biological metabolisms and chemical oxidation processes in which the redox metal oxo moieties at the high oxidation state, M^{n+}=O, were first proposed to serve as the key active intermediates in a wide range of these oxidative events including electron transfer, hydrogen atom transfer and oxygen transfer, etc.[1, 2] Later, the metal hydroperoxide moieties, M^{n+}-OOH which were early suspected to be the precursors in generating the corresponding active M^{n+}=O moieties, were recognized to be capable of oxidizing many organic compounds such as olefins and sulfides.[3] Even the metal hydroxo functional groups, a hydroxide anion ligated to the redox metal ion, M^{n+}-OH, have also been realized to be able to serve as the key active intermediates in certain oxidation events.[4] Up to now, the scope of the metal ions based active species in versatile oxidations has extended from the M^{n+}=O to M^{n+}-OOH, and M^{n+}-OH moieties.

In artificial redox catalysts, one may argue that the occurrence of the M^{n+}=O, M^{n+}-OH or M^{n+}-OOH as the active intermediate in different oxidation reactions is quite random, and highly catalysts dependent. In many cases, they may simultaneously exist in one process, which causes the low selectivity of expected products. However, in nature, the redox enzyme's choice on them must be extremely strict, because the enzymatic reactions are highly specific. In another word, the occurrence of them in different categories of enzymes is highly dependent on their distinct reactivity differences, not because of their similarities. For examples, the compound I intermediate in P450 enzymes is in an iron(IV) oxo form[5] whereas it is in an iron(III) hydroxo rather than the corresponding oxo form in lipoxygenases.[4] Up to now, the redox mechanisms of these enzymes are not fully understood yet, and the control of the above mentioned active intermediates in different redox catalysts is very difficult. Apparently, clarifying the oxidative reactivity similarities and differences of these active moieties in oxidations would definitely help the elucidation of the enzymatic mechanisms, and benefit the rational design of selective redox catalysts.

For the M^{n+}=O and M^{n+}-OH moieties, the viable difference between them is their different protonation state which leads to

their different functional metal-oxygen bond order (double *vs* single bond) with different net charge. That is, protonation of the M^{n+}=O functional group to form the M^{n+}-OH moiety would increase one unit of the positive charge on the active intermediate. These changes would obviously affect the related physicochemical properties and oxidative reactivity of the central metal ions. Clarifying their reactivity relationships in oxidations would benefit the understanding of the origins of redox enzymes' choice on them. This review will first summarize the reactivity of the active M^{n+}=O and M^{n+}-OH moieties in oxidations with comparing their similarities and differences in different oxidation processes. Based on these discussions, it leads to summarize how the oxidative reactivity of a redox metal ion changes with the change of its physicochemical properties such as metal-oxygen bond order, net charge and redox potential. Finally, its implications in understanding the enzymatic mechanisms, explaining elusive oxidation phenomena, and designing selective redox catalysts will be presented.

2 The oxidative reactivity of active metal oxo moieties

Redox metal oxo moieties, M^{n+}=O, have been long recognized to serve as the key active intermediate in most biological oxidation events. One well known example is the (Porp)Fe^{IV}=$O^{+\bullet}$ (Porp: Porphyrin), named compound I, in P450 enzymes, which has attracted much attentions due to its vital roles in a variety of biologically important processes such as metabolism and immune defense. These M^{n+}=O moieties also play the central roles in versatile oxidation processes employed in chemical industry and laboratory synthesis. Due to their significant roles in biological and chemical oxidation processes, the oxidative reactivity of these M^{n+}=O moieties including hydrogen atom abstraction, oxygen atom transfer and electron transfer has been extensively investigated. Here, to compare the reactivity of the M^{n+}=O with its corresponding M^{n+}-OH moiety, the reactivity of the active M^{n+}=O moieties from different metal ions will be briefly summarized in this section.

2.1 Hydrogen atom transfer reactivity of the metal oxo moieties

Hydrogen atom transfer is among the most attractive topics in chemistry, which provides promise of understanding the fundamental oxidation events in nature and chemical industries. It has been believed that the redox metal ions play the crucial roles in these hydrogen transfer reactions, and an oxygen rebound mechanism, coined by Groves, was applied to elucidate the reaction mechanisms.[6] In this mechanism, the active M^{n+}=O moiety, generated by oxidizing of redox catalyst with oxidant, abstracts a hydrogen atom from the substrate to yield a substrate radical (R•) with the reduced $M^{(n-1)+}$-OH. Then, the $M^{(n-1)+}$-OH moiety rebinds the OH group back to the radical intermediate to produce the hydroxylation product (Scheme 1).[7] In a typical rate determining hydrogen abstraction step, the value of the H/D kinetic isotope effect (KIE) is generally in the range of 2~7, which has been commonly acknowledged as a criteria of whether hydrogen abstraction serving as the rate determining step.

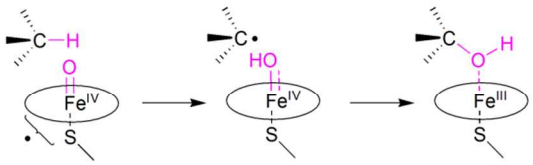

Scheme 1 Hydroxylation of alkane with Fe(IV)=O following oxygen rebound mechanism. Reprinted with permission from ref. 7. Copyright 2004 The American Association for the Advancement of Science.

The hydrogen abstraction capability of an active M^{n+}=O moiety can be evaluated by the method introduced by Bordwell and Mayer. After hydrogen abstraction, the bond dissociation free energies of O-H bond ($BDFE_{OH}$) in the generated $M^{(n-1)+}$-OH group is defined by the redox potential of the M^{n+}=O moiety with the pK_a value of its reduced $M^{(n-1)+}$-OH as demonstrated in Eq. 1, where C is a constant. Accordingly, the thermodynamic driving force of a M^{n+}=O moiety in hydrogen abstraction is equal to the $BDFE_{OH}$ value as defined in Eq 1.[2]

$$BDEF_{OH} = 23.06E_{1/2} + 1.37pK_a + C \qquad \text{Eq. 1}$$

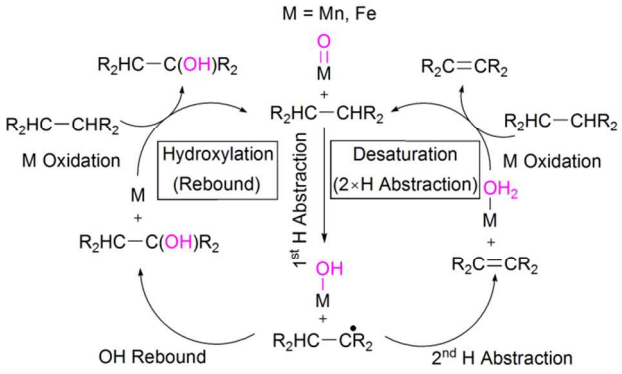

Scheme 2 Proposed mechanisms for hydroxylation and desaturation by metal oxo species. Reprinted with permission from ref. 8. Copyright 2010 American Chemical Society.

After hydrogen abstraction by the M^{n+}=O moiety, the generated substrate radical (R•) could go through two pathways to form either hydroxylation or desaturation product. While the hydroxylation product is formed by oxygen rebound mechanism as illustrated in Scheme 1, the desaturation product is generated through second hydrogen abstraction from the substrate radical by the reduced $M^{(n-1)+}$-OH moiety or another M^{n+}=O moiety (Scheme 2). Through experimental tests and DFT calculations with several manganese models, Brudvig and co-workers revealed that the Mn^{V}=O moiety can oxidize dihydrophenanthrene by either desaturation or hydroxylation, while the resulting Mn^{IV}-OH intermediate is capable of promoting not only OH rebound (hydroxylation) but also a second H abstraction adjacent to the first which leads to desaturation.[8] The capability of the Mn^{IV}-OH moiety to perform

hydrogen abstraction in addition to OH rebound was attributed to its radical character on the oxygen atom. Moreover, the radical character of the oxygen is located on its p orbital perpendicular to the MnOH plane, thus the orientation of the substrate radical with respect to this plane determines either hydroxylation or desaturation reaction occurs.

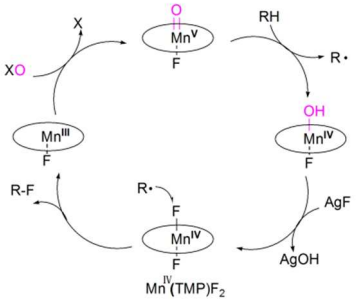

Scheme 3 Catalytic cycle of Mn(TMP)Cl mediated C-H fluorination reactions. Reprinted with permission from ref. 9. Copyright 2012 The American Association for the Advancement of Science.

In addition to hydroxylation and desaturation, Groves recently disclosed that, under certain conditions, hydrogen abstraction by M^{n+}=O moieties can also lead to oxidative C-H fluorination. In the presence of fluoride ion, they found that the Mn(TMP)Cl complexes can selectively catalyse alkyl fluorination with PhIO as oxidant, and the catalytic cycle follows that: the *in situ* generated O=Mn^{V}(TMP)F species abstracts the hydrogen atom from the substrate to produce a C-centred radical, and the HO-Mn^{IV}-F intermediate is formed as usual (Scheme 3, TMP: 5,10,15,20-tetramesitylporphyrinato dianion). Then the OH group can be replaced by an external F^- anion to generate the *trans*-difluoro-Mn^{IV}(TMP) species, F-Mn^{IV}-F, which can rebind the F^- anion to the substrate radical to achieve C-H fluorination. The structure of *trans*-difluoro-Mn^{IV}(TMP) has been identified by single crystal X-ray diffraction as well. DFT calculations show that F atom transfers from *trans*-difluoro-Mn^{IV}(TMP) to a cyclohexyl radical was predicted to occur with a surprisingly low activation barrier of only 3 kcal/mol, which is similar to the oxygen atom rebound barrier for hydroxylation reactions catalyzed by O=Mn^{V}(porphyrins).[9]

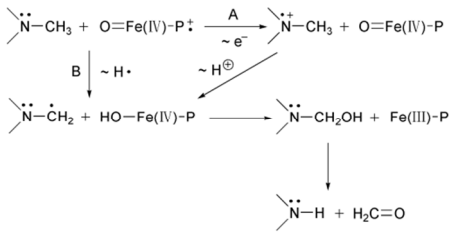

Scheme 4 The hydrogen atom transfer (HAT) *vs* electron/proton transfer (ET/PT) mechanism of dealkylation by P450s. Reprinted with permission from ref. 10. Copyright 1995 American Chemical Society.

The oxidative dealkylation is an important biotransformation reaction catalyzed by a number of metalloenzymes, and clarifying its catalytic mechanism is also crucial to the understanding of the metabolism of xenobiotics compounds. In P450 enzymes mediated amine oxidations, it has been proposed that dealkylation proceeds by either electron/proton transfer (ET/PT) mechanism or hydrogen atom abstraction mechanism, and the H/D KIE in dealkylation has been applied to distinguish two mechanisms (Scheme 4). For this issue, through comparing the H/D KIE of dealkylation by t-BuO• with a series of P450 enzymes, Dinnocenzo and co-workers found that they have the identical KIE values, thus providing compelling evidence to support that dealkylation by P450s proceeds by hydrogen atom abstraction.[10] If the dealkylation proceeded by electron/proton transfer, the KIE will demonstrate a bell-shaped effect with the change of the pK_a of the radical cations, as well as Fe^{3+}(Phen)/pyridine mediated dealkylation which is a classical electron/proton process.

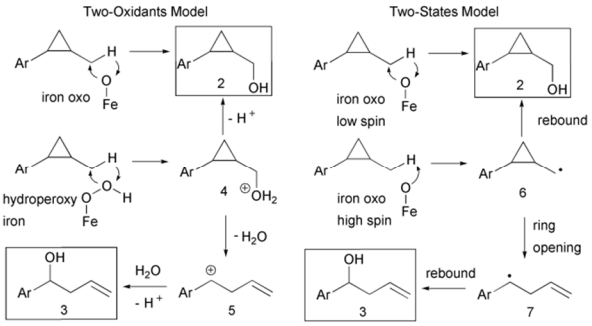

Scheme 5 Oxidation of *trans*-2-(p-trifluoromethylphenyl)cyclopropylmethane (**1**) following multiple reaction pathways: Comparing the two-oxidants and two-states models. Reprinted with permission from ref. 11. Copyright 2004 American Chemical Society.

In the past decades, although it has been well accepted that the Fe^{IV}=$O^{+\bullet}$ form of the compound I in P450s serves hydrogen abstraction in biological metabolisms, and many synthetic models containing M^{n+}=O functional group have also confirmed its hydrogen abstraction reactivity, the accumulated clues have also pointed out that the hydroxylation reactions are very complicated, and the experimental results sometimes cannot be explained by a single reaction pathway. Currently, it has put forward at least two distinct models to rationalize P450-catalyzed hydroxylation including "two-oxidants" and "two-states" models. In two-oxidants model, Newcomb and co-workers suggested that, in addition to the compound I, its precursor, iron(III) hydroperoxide intermediate, Fe^{III}-OOH, may serve as a second oxidant in hydrogen abstraction step. As shown in Scheme 5, Fe^{IV}=O moiety can react with *trans*-2-(*p*-trifluoromethylphenyl)cyclopropylmethane (**1**) to produce alcohol (**2**) directly by a typical oxygen rebound mechanism. While the second oxidant, the Fe^{III}-OOH moiety will insert OH^+ into the substrate **1** to give protonated alcohol intermediate (**4**) initially, then the product **2** was generated by deprotonation of **4**. Meanwhile, the ring-opened product **3** can also be formed via deprotonation of the cationic intermediate **5** which was formed by re-arrangement of the intermediate **4** after dehydration.[11] This "two-oxidants" model was based on

Newcomb and co-workers' analysis on the intramolecular and intermolecular kinetic isotope effects in P450s mediated hydroxylations. On the other hand, based on DFT calculations for a series of nonheme iron(IV) oxo complexes catalyzed alkane hydroxylation, Shaik and co-workers proposed a "two-states" model for hydroxylation.[12] The authors found that both low-spin and high-spin states of Fe^{IV}=O moiety are energetically accessible. The low-spin state of Fe^{IV}=O may react by an insertion reaction to produce **2**, while the high-spin state of Fe^{IV}=O reacts by a hydrogen atom abstraction reaction that gives the radical intermediate **6**, then produces **2** by a direct rebound step, or gives **3** via ring opening followed by a rebound step. Both models accommodate the Fe^{IV}=O insertion reaction, and the difference involves the identity of the "other" oxidant: Fe^{III}-OOH or a second spin state of Fe^{IV}=O. Up to now, the arguments between two mechanisms still exist, and more convincible evidence is essential to support either of them.

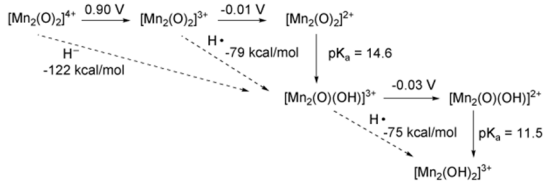

Scheme 6 Redox potentials (*vs* $Cp_2Fe^{+/0}$), pK_a values, H· and H^- affinities of $[(phen)_2Mn^{IV}(\mu\text{-}O)_2Mn^{IV}(phen)_2]^{4+}$ in MeCN. Reprinted with permission from ref. 13. Copyright 2002 American Chemical Society.

Besides hydrogen atom abstraction, hydrogen transfer could also happen as a hydride transfer. Fundamentally, the hydride transfer is equal to transferring of two electrons and one proton, while hydrogen atom transfer involves the transfer of one electron and one proton. Mayer and co-workers evaluated the thermodynamic ability of the manganese oxo dimmers, including $[(phen)_2Mn^{IV}(\mu\text{-}O)_2Mn^{IV}(phen)_2]^{4+}$ (**$[Mn_2(O)_2]^{4+}$**), $[(phen)_2Mn^{IV}(\mu\text{-}O)_2Mn^{III}(phen)_2]^{3+}$ (**$[Mn_2(O)_2]^{3+}$**), and $[(phen)_2Mn^{III}(\mu\text{-}O)(\mu\text{-}OH)Mn^{III}(phen)_2]^{3+}$ (**$[Mn_2(O)(OH)]^{3+}$**), in accepting e^-, H•, or H^- by its redox potentials and pK_a values (Scheme 6). As they found, the **$[Mn_2(O)_2]^{3+}$** moiety tends to transfer hydrogen through hydrogen atom abstraction process because it is capable of generating strong O-H bond (79 kcal/mol). Since it is not a good outer-sphere oxidant, electron transfer is not favourable. In contrast, **$[Mn_2(O)_2]^{4+}$** moiety does not react via hydrogen atom abstraction which requires accepting both an electron and a proton, and **$[Mn_2(O)_2]^{3+}$** has low basicity. However, it can react either by electron transfer or by accepting a hydride to form stable **$[Mn_2(O)(OH)]^{3+}$**. In alkylaromatic compound oxidations, the authors observed that there is a large thermodynamic bias for **$[Mn_2(O)_2]^{4+}$** to accept a hydride rather than an electron from toluene (31 kcal/mol), strongly indicating that **$[Mn_2(O)_2]^{4+}$** prefers a hydride transfer mechanism. However, in the case of *p*-methoxyltoluene, even that its oxidation by **$[Mn_2(O)_2]^{4+}$** through hydride transfer is energetically 24 kcal/mol more favourable than electron transfer, the reaction does proceed by electron transfer, and this preference was attributed to its substantially smaller intrinsic barrier.[13] In investigating the Mn(TMP) oxo mediated electron transfer and hydride transfer, Fukuzumi and Nam also found that the reaction is substrate dependent. Using NADH analogs as substrates, $(TMP)Mn^{IV}$=O would first disproportionate to form $[(TMP)Mn^{III}]^+$ and $[(TMP)Mn^{V}=O]^+$, and the later then performs hydride transfer from NADH analog to form $[(TMP)Mn^{III}(OH)]$. In the case of ferrocene derivative substrates, the $(TMP)Mn^{IV}$=O would be directly reduced through electron transfer, since the disproportionation equilibrium of $(TMP)Mn^{IV}$=O is unfavorable in this case (Scheme 7).[14] These studies have provided valuable mechanistic insights into the tuning of reaction pathways depending on substrates and reaction conditions.

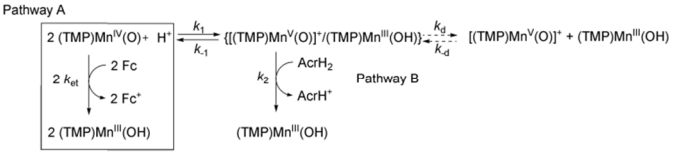

Scheme 7 Proposed mechanisms for hydride transfer reactions by $(TMP)Mn^{IV}$=O. Reprinted with permission from ref. 14. Copyright 2009 American Chemical Society.

2.2 Oxygen atom transfer reactivity of the metal oxo moieties

Oxygen atom transfer is another important process in biological and chemical oxidations mediated by versatile active M^{n+}=O moieties, and olefin epoxidation is a typical modelling reaction for this study. Groves even found that an iron porphyrin complex, $(TPP)Fe^{III}Cl$ (TPP: chloro-α,β,γ,δ-tetra-phenylporphinato), could catalyse transferring of oxygen atom from iodosylbenzene to both olefins and paraffins, thus coined the classic oxygen rebound mechanism as shown in Scheme 8: the reduced form of the iron center initially receives oxygen from oxidant (**:**O-X) and produces the Fe^{IV}=O species. Then, the Fe^{IV}=O species transfers the activated oxygen atom to the substrate, olefin or paraffin, by oxygenation.

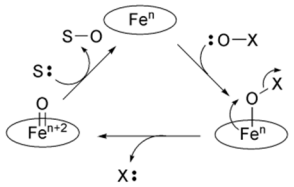

Scheme 8 Oxygen atom transfer by iron oxo species following oxygen rebound mechanism (modified from ref. 6).

The key experimental evidence to support that M^{n+}=O group functions as the active intermediate in olefin epoxidation comes from isotope labelling studies. In Groves' studies using Mn^{III}(TMPyP) complex as catalyst (TMPyP: tetra-N-(methylpyridyl)porphyrinato), its oxidation by $KHSO_5$ oxidant gives Mn^{V}(TMPyP)(O) intermediate which can exchange oxo with ^{18}O-water to form Mn^{V}(TMPyP)(^{18}O). Next, it was identified that the ^{18}O can be subsequently incorporated into olefin, forming the ^{18}O-epoxide product, thus the reactive

(TMPyP)Mn^{V}=O was established as the active intermediate in olefin epoxidation (Scheme 9).[15]

In olefin epoxidation reaction, the popular oxidants include H_2O_2, PhIO, and peracid, etc., whereas dioxygen was seldom employed as oxidant because it generally requires a co-reductant for its activation. Using Ru^{II}(TMP)Cl_2 as catalyst, Che and co-workers introduced a rare example of olefin epoxidation by dioxygen in base, and the generated epoxide is then *in situ* isomerized to aldehyde.[16] Examined by ^{1}H NMR, the reaction was found to have an induction period, followed by dioxoruthenium(VI) intermediate formation through Ru^{II}(TMP)Cl_2 oxidation with dioxygen. Then the *in situ* generated dioxoruthenium(VI) intermediate initializes the olefin epoxidation. The presence of the base plays a key role in isomerizing of epoxide to aldehyde. Such a selective reaction of tandem Epoxidation-Isomerization pathway using dioxygen as oxidant complements the conventional Wacker oxidations that usually afford methyl ketones.

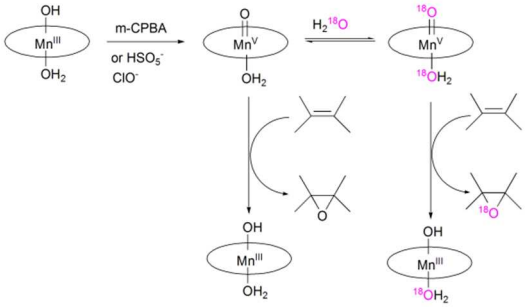

Scheme 9 The isotope labelling evidence for oxygen rebound mechanism (modified from ref. 15).

In addition to the Fe^{IV}=O, Mn^{V}=O, Ru^{VI}=O species illustrated above, other redox M^{n+}=O moieties including Cr^{V}=O, Re^{VII}=O and Mo^{VI}=O, etc., have also been proposed to serve as the key active intermediates in oxygen transfer process. Molybdenum enzymes represent a great family of metalloenzymes which mediate the critical oxidation processes in metabolism of C, N and S by all forms of life. A number of synthetic molybdenum complexes containing two or more sulfur ligands have been prepared and some of them were tested as oxygen transfer catalysts. Holm and co-workers even demonstrated an example of oxygen transfer from the synthetic Mo(VI) complex to triarylphosphine (Scheme 10). In DMF solution, the synthetic $Mo^{VI}(O)_2$(L-NS_2) complex (L-NS_2:2,6-bis(2,2-diphenyl-2-mercaptoethyl)pyridine) can achieve oxygen transfer from the Mo^{VI}=O to (p-$FC_6H_4)_3$P, in which the Mo^{VI} is reduced to the corresponding Mo^{IV} form. Then, the reduced Mo^{IV} ion can be re-oxidized by N-oxide or sulfoxide again. As an example of catalysis, this molybdenum complex could achieve catalytic oxygen transfer from N-oxide to triarylphosphine with over 100 turnovers in 15 h.[17]

Oxidation of organic sulfides is another category of oxygen transfer process, which represents an important biological metabolism in nature. Sulfide oxidations catalyzed by redox enzymes and synthetic catalyst are known to proceed by both oxygen atom transfer and electron transfer mechanisms. Collins and co-workers even carried out a detailed dynamic study on sulfide oxidation by their Fe(TAML) catalyst (TAML: tetraamido macrocyclic ligand). It was found that the reaction follows saturation kinetics in p-XC_6H_4SMe with electron-rich substrates (X = Me, H), but changes to linear kinetics with electron-poor substrates (X = Cl, CN) due to that the sulfide affinity to iron decreases. The ratio of oxygen transfer rate (k^{OAT}_{obs})/electron transfer rate (k^{ET}_{obs}) is calculated to be 1.9 (X = Me), 0.88 (X = H), 0.57 (X = Cl) and 0.20 (X = CN) respectively, suggesting that the oxygen transfer dominates only slightly over electron transfer for the electron-rich sulfides in the studied ArSMe series, and electron-withdrawing groups induce the sulfides to react predominantly via electron transfer.[18]

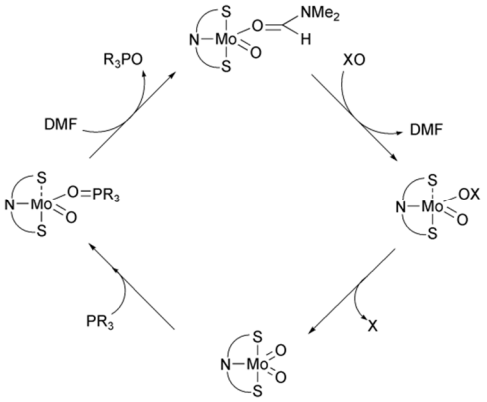

Scheme 10 Oxygen atom transfer by molybdenum complex (modified from ref. 17).

Recently gold has been found to be surprisingly active and selective to a broad scope of organic synthetic transformations, thus captures the extensive attentions in community. Corma and co-workers found that a chiral Au(III) complex (L$AuCl_3$, L: 2,6-bis[(4R)-phenyl-2-oxazolin-2-yl]pyridine) can enantioselectively epoxidize olefins with dioxygen. Isotopic $^{18}O_2$ labelling experiments reveal that the ^{18}O has been incorporated into the epoxide product, indicating that the gold complex can directly activate dioxygen and transfer oxygen to olefin by a non-radical pathway.[19] Upon adding NaOCl to the gold complex**,** a new band at 460 nm in UV-Vis spectrum and one at 262 cm^{-1} in Raman spectrum was assigned to a gold-oxygen vibration by the authors, indicating that a gold oxo or peroxo species has been formed under oxidation conditions. Combined with other characterizations, it leads the authors to propose an Au^{III}=O moiety serves as the active intermediate in olefin epoxidation as well as other M^{n+}=O moieties. However, further characterization and experimental data are still needed to evidence the existence of Au^{III}=O species in catalytic oxidation.

2.3 Electron transfer reactivity of the metal oxo moieties

Electron transfer is the most fundamentally oxidative process in nature in which a great family of peroxidases plays the key

roles. Chloroperoxidase (CPO) is a well-studied peroxidase which is capable of degrading chlorophenols through electron transfer. In H_2O_2 dependent dehalogenation of chlorophenols by CPO, Dawson and co-workers found that monohalogenated phenol, i.e., *p*-chlorophenol, as substrate would generate a dimmer as the major product with minor *p*-benzoquinone formation, indicating that a free radical intermediate is produced and the dehalogenation involves an electron transfer process rather than direct oxygen atom insertion. Based on these clues, the authors suggested a CPO catalyzed dehalogenation mechanism as shown in Scheme 11. The CPO Compound I，an $Fe^{IV}=O^{+\bullet}$ form of oxidant first oxidizes the halophenol substrates through electron transfer to form a phenoxy radical and CPO Compound II，an $Fe^{IV}=O$ species. Dimerization can occur through the resonance form of the phenoxy radical if there was no substituent on the carbon ortho to the phenol oxygen. In the case of halophenol dehalogenation, further one electron oxidation of the phenoxy radical yields $Fe^{IV}=O$ and a cation intermediate. The cation intermediate then reacts with water followed by deprotonation and elimination of HCl, which results in formation of benzoquinone product.[20]

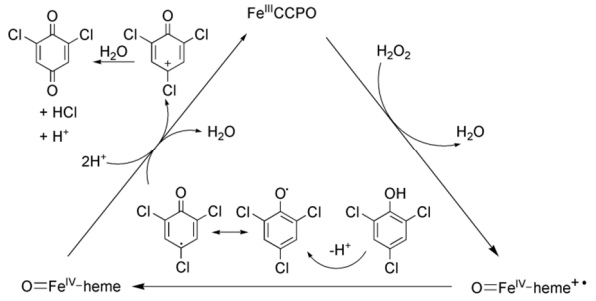

Scheme 11 Proposed mechanism of H_2O_2 dependent dehalogenation of chlorophenols by chloroperoxidase (CPO). Reprinted with permission from ref. 20. Copyright 2007 American Chemical Society.

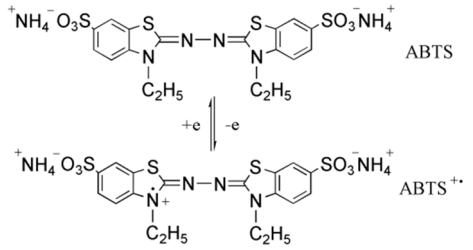

Scheme 12 Chemical structures of ABTS and $ABTS^{+\bullet}$ species and their electron transfer.

ABTS (2,2'-azino-di-(3-ethylbenzthiazoline-6-sulphonic acid) is a classic reagent to probe the electron transfer reaction, because after one electron transfer, the generated $ABTS^{+\bullet}$ demonstrates a distinctly different UV-Visible absorbance from that of original ABTS (Scheme 12). Eldik and co-workers found that both $Fe^{IV}=O^{+\bullet}$ and $Fe^{IV}=O$ intermediates, the analogs of compound I and II in peroxidases,[21] can be generated by oxidizing the water-soluble octa anionic porphyrin $Na_7[(P_8^-)Fe^{III}]$ with H_2O_2 under different pH conditions (P_8^-: $5^4,10^4,15^4,20^4$-tetra-*tert*-butyl-$5^2,5^6,15^2,15^6$-tetrakis[2,2-bis(carboxylato)ethyl]-5,10,15,20-tetraphenylporphyrin). Using ABTS as a substrate, both iron(IV) oxo intermediates have been observed to achieve one electron transfer from ABTS to give the characteristic absorbance of $ABTS^{+\bullet}$ species, thus confirms their electron transfer capability.

Fukuzumi and Nam applied the Marcus theory of adiabatic outer-sphere electron transfer to explain the $M^{n+}=O$ mediated electron-transfer. The authors found that the nonheme Mn(IV) oxo complex $[(Bn\text{-}TPEN)Mn^{IV}(O)]^{2+}$ (Bn-TPEN: N-benzyl-N,N',N'-tris(2-pyridylmethyl)-1,2-diaminoethane) can oxidize the electron donor dibromoferrocene (Br_2Fc), while under the identical conditions no electron transfer can be observed from Br_2Fc to $[(Bn\text{-}TPEN)Fe^{IV}(O)]^{2+}$, indicating that the $Mn^{IV}=O$ moiety is a stronger one-electron oxidant than the corresponding $Fe^{IV}=O$ with this Bn-TPEN ligand.[22] The authors rationalized it by the fact that the apparent one electron reduction potential, E_{red}, of $[(Bn\text{-}TPEN)Mn^{IV}(O)]^{2+}$ is +0.78 V (*vs* SCE), significantly more positive than that of corresponding $[(Bn\text{-}TPEN)Fe^{IV}(O)]^{2+}$ (+0.49 V *vs* SCE). The second-order rate constants of electron transfer from ferrocene derivatives to $[(Bn\text{-}TPEN)Mn^{IV}(O)]^{2+}$, k_{et}, were also determined. As shown in Fig. 1, The driving force dependence of electron transfer ($-\Delta G_{et}$) against the rate constants (log k_{et}) is well fitted by the solid line in light of the Marcus theory of adiabatic outer-sphere electron transfer (Eq. 2), where Z is the collision frequency, K_b is the Boltzmann constant, T is the absolute temperature, and λ is the reorganization energy of ET. The λ value is determined to be 2.37 eV, which is similar to those determined for electron transfer reduction of nonheme iron(IV) oxo complexes, indicating that one electron reduction of high-valent $M^{n+}=O$ moieties generally requires large reorganization energy, probably due to significant elongation of $M^{n+}=O$ bonds upon one electron reduction.[1]

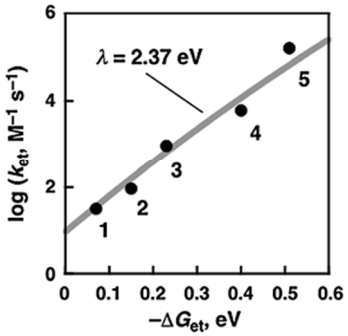

Fig. 1 Driving force of the ET ($-\Delta G_{et}$) dependence of rate constants (log k_{et}) from one-electron donors (In this figure, **1**: Br_2Fc, **2**: acetylferrocene, **3**: bromoferrocene, **4**: ferrocene, **5**: dimethylferrocene) to $[(Bn\text{-}TPEN)Mn^{IV}(O)]^{2+}$ in CF_3CH_2OH-MeCN (1:1,v/v) at 273 K. The gray line is the Marcus line calculated with λ value of 2.37 eV. Reprinted with permission from ref. 22. Copyright 2012 Royal of Social Chemistry.

$$k_{et} = Z\exp[-(\lambda/4)(1+\Delta G_{et}/\lambda)^2/k_B T] \quad \text{Eq. 2}$$

Although dealkylation may proceed by hydrogen atom abstraction as stated in section 2.1, the debated issue is that the primary step of the oxidation sequence may also proceed by electron transfer. In electron transfer mechanism, a single electron oxidation of the heteroatom gives a radical cation which undergoes subsequent deprotonation (PT) at a C-H bond on the carbon adjacent to the hetero atom (Scheme 13), forming a α-carbon centred neutral radical. Alternatively, a hydrogen atom abstraction mechanism involves a homolytic breaking of a C-H bond followed by a rebound step, which has been discussed in section 2.1. Fornarini and co-workers investigated gas-phase reactions of $[(TPFPP)Fe^{IV}=O^{+\bullet}]^+$ (TPFPP : meso-tetrakis(pentafluorophenyl)porphinatodianion) with different tertiary amines using ESI-FT-ICR mass spectrometry.[23] The gas phase reaction can avoid the influence of bulky solvent environment in enzymatic pocket which may remarkably affect the reactivity of the active species. The authors found that the reaction appears to be initiated by an electron transfer event for the majority of the tested amines. The primary electron transfer pathway yields $(TPFPP)Fe^{IV}=O$ and the amine radical cation product, followed by a hydrogen atom transfer or a stepwise proton transfer and electron transfer route forming $[(TPFPP)Fe^{III}\text{-}OH]$ and iminium ion (Scheme 13). Furthermore, the authors found that electron transfer efficiency can be well correlated with the ionization energy of investigated amines.

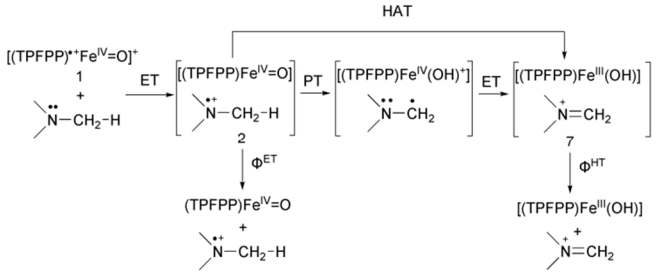

Scheme 13 Proposed reaction pathway of $[(TPFPP)Fe^{IV}=O^{+\bullet}]^+$ oxidative N-dealkylation. Reprinted with permission from ref. 23. Copyright 2008 American Chemical Society.

In addition to $(Porp)Fe^{IV}=O^{+\bullet}$ as chemical models of P450 enzymes, nonheme iron(IV) oxo complexes have also been studied in N-dealkylation reactions. Nam and co-workers compared the dealkylation reaction of *in situ* generated nonheme and heme iron(IV) oxo complexes.[24] Their dealkylation rates are observed linearly correlating with the σ_p of *para*-substituted dimethylanilines in Hammett plot, and particularly, the plot of $\log k_{obs}$ against the one electron oxidation potentials of substituted substrates provides a good linear correlation with large negative slopes, which apparently suggests the rate-limiting electron transfer from substrates to the iron(IV) oxo species. Further evidence came from the dealkylation of *p*-chloro-N-ethyl-N-methylaniline in which N-demethylation is greatly favoured over N-deethylation. This tendency is consistent with that, in proton transfer from the amminium radical to the $Fe^{IV}=O$ species, the deprotonation of the methyl group is preferred over the ethyl methylene, because the acidity of the methyl proton is higher than that of the ethyl one. If the N-dealkylation initiates via a hydrogen atom abstraction mechanism, the formation a deethylated product should be a preferred pathway owing to the weak methylene C-H bond strength (about 3 kcal/mol less than the methyl C-H bond strength). Taken together, both hydrogen atom abstraction and electron transfer mechanisms have been proposed for $M^{n+}=O$ moieties mediated N-dealkylation with convincible evidence. Possibly both mechanisms may independently happen with different catalysts, otherwise, they may competitively occur to a different extent.

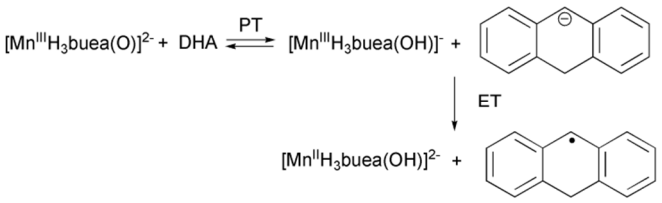

Scheme 14 Proposed PT/ET mechanism for the reaction of $[Mn^{III}H_3buea(O)]^{2-}$ with 9,10-dihydroanthracene. Reprinted with permission from ref. 25. Copyright 2009 American Chemical Society.

Besides the ET-PT pathway as described above, the PT-ET pathway has also been reported in $M^{n+}=O$ mediated hydrogen transfer. Borovik and co-workers investigated the reactions of 9,10-dihydroanthracene (DHA) with two manganese oxo complexes, $[Mn^{III}H_3buea(O)]^{2-}$ and $[Mn^{IV}H_3buea(O)]^-$, (H_3buea: tris[(N-*tert*-butylureaylato)-N-ethylene]aminato).[25] Dynamic studies revealed that the observed second order rate constant difference (0.48 M^{-1} cm^{-1} for $[Mn^{III}H_3buea(O)]^{2-}$ and 0.026 M^{-1} cm^{-1} for $[Mn^{IV}H_3buea(O)]^-$) is related to the basicity of the oxo ligands in two manganese complexes, which leads the authors to suggest different mechanisms for two complexes. The large difference between the pK_a values (ΔpK_a~15) of the C-H bonds in DHA (pK_a=30) and $[Mn^{IV}H_3buea(OH)]^-$ (pK_a~15) makes the $[Mn^{IV}H_3buea(O)]^-$ to react via the direct hydrogen atom abstraction in which both DHA and the Mn(IV) complex appear in the transition state together. While for the $[Mn^{III}H_3buea(O)]^{2-}$, the oxo ligand is significantly more basic (pK_a~28.3 in $[Mn^{III}H_3buea(OH)]^-$) than the hydroxo moiety in $[Mn^{IV}H_3buea(OH)]^-$ (pK_a~15), thus a two-step mechanism may occur in which the proton transfer happens prior to electron transfer (Scheme 14).

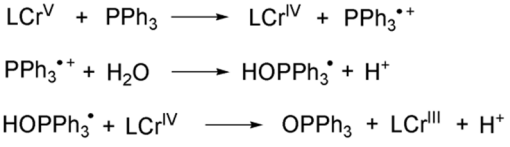

Scheme 15 Proposed mechanism for the reaction of $LCr^V=O$ and PPh_3. Reprinted with permission from ref. 26. Copyright 2003 American Chemical Society.

The chromium complex with macrocyclic ligand has also been observed to perform electron transfer reactions. Bakac and co-workers showed that a strongly oxidizing LCr^{V}=O (L: *trans*-[14]aneN_4), generated from LCr^{III}-OOH, reacts with triarylphosphines exhibiting a 1:1 stoichiometry and mixed second-order kinetics, and the Hammett plot for the reaction gives the slope (ρ) of -0.69, consistent with the electrophilic character of Cr(V).[26] When LCr^{V} was generated from $[LCr^{18}O^{18}OH]^{2+}$, it was found that the product $OPPh_3$ contains no labelled oxygen. Since none of the chromium species can exchange oxygen with water on the time scale of this oxygenation process, it suggests electron transfer as the most likely mechanism as showing in Scheme 15. On the other hand, $[L(H_2O)Cr^{18}O^{18}OH]^{2+}$ reacted with PPh_3 and produced $^{18}OPPh_3$ in the presence of either $^{18}O_2$ or $^{16}O_2$, clearly demonstrating an oxygen atom transfer mechanism. This investigation of comparing oxidation pathway of LCr^{V}=O and $[L(H_2O)CrOOH]^{2+}$ also provides clues to the reactivity differences of the active M^{n+}=O with its corresponding M^{n+}-OOH moieties.

2.4 Oxidative reactivity of polyoxometalates

Polyoxometalates (POMs), consists of three or more transition metal anions linked together by shared oxygen atoms to form a framework is another common structure that contains M=O moiety. POMs have stimulated many current research activities in a broad range of oxidation process because their reactivity and acidities can be finely tuned by choosing the constituent elements and counter cations. For example, in the common Keggin structure, $[X^{n+}W_{12}O_{40}]^{(8-n)-}$, the central hetero atom, X^{n+}, can be a list of elements in the periodic table, and 1, 2 or 3 of the original tungsten atoms (usually a terminal $[W=O]^{4+}$ unit) can be replaced with other p or d block elements (Scheme 16).

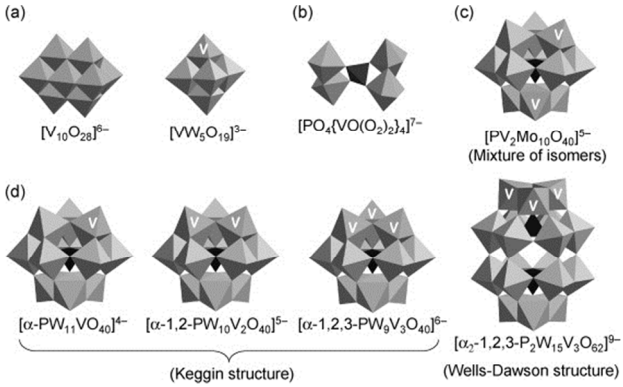

Scheme 16 Polyhedral representations of various kinds of vanadium-based POMs. (a) Isopolyoxometalates, (b) peroxometalate, (c) mixed-addenda heteropolyoxometalate, and (d) transition metal-substituted heteropolyoxometalates. Reprinted with permission from ref. 27. Copyright 2011 Elsevier.

Because POMs catalysed oxidations of hydrocarbon have been comprehensively reviewed elsewhere,[27] only a few recent examples are introduced here. Neumann and co-workers found that $H_5PV_2Mo_{10}O_{40}$ can catalyse sulfide oxygenation to the corresponding sulfoxides by an electron transfer-oxygen transfer (ET-OT) mechanism.[28] In this process, an outer-sphere ET reaction between R_2S and $H_5PV_2MO_{10}O_{40}$ leads to an ion pair (step (a) in Scheme 17), followed by an OT reaction that removes VO^{2+} from POMs. The sulfoxide is finally liberated with the formation of the reduced $H_7PV^{IV}{}_2Mo_{10}O_{40}$ (step (c)). Besides the above-mentioned traditionally catalytic oxidations, POMs have recently been recognized as tuneable catalysts in biomass valorization.[29]

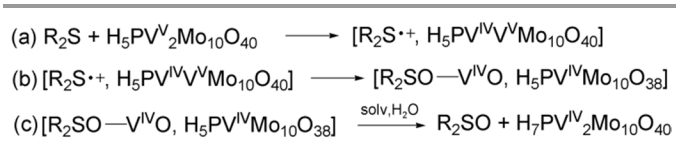

Scheme 17 Proposed reaction pathway for ET-OT oxidation of Sulfides catalysed by $H_5PV_2Mo_{10}O_{40}$. Reprinted with permission from ref. 28. Copyright 2010 American Chemical Society.

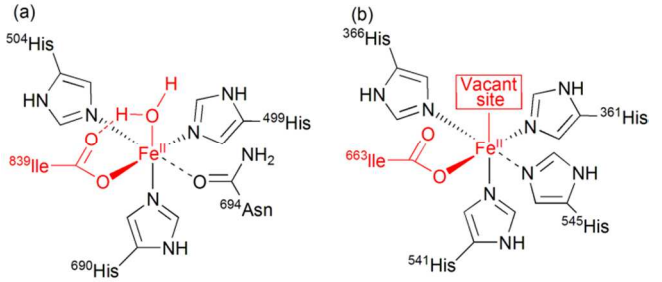

Scheme 18 Core structure of the active site in (a) soybean lipoxygenase-1 and (b) 15-rabbit lipoxygenase. Reprinted with permission from ref. 31. Copyright 2002 American Chemical Society.

3 The oxidative reactivity of active metal hydroxo and its comparison with the corresponding metal oxo moieties

While the M^{n+}=O moieties are recognized as the key active species in most of biological and chemical oxidation processes, the increasing clues have also revealed that the active metal hydroxo moiety, M^{n+}-OH, traditionally regarding as a hydroxide anion ligated to the metal ion, may also serve as the active species in certain cases.[7] In lipoxygenases, it has been found that it is an iron(III) hydroxo moiety, not an iron(III) oxo, functions as the key intermediate to abstract hydrogen atom from the unsaturated fatty acids which further proceeds rearrangement and dioxygen trapping to form the alkyl hydroperoxide products.[4] Beside Fe^{III}-OH moiety, Oliw even disclosed a manganese lipoxygenase in the fungus *Gäumannomyces graminis* which has a Mn^{III}-OH moiety to serve hydrogen abstraction as well as Fe^{III}-OH in iron lipoxygenases.[30] The resolved crystal structures disclosed that the active sites of plant and animal lipoxygenases are different. In soybean lipoxygenase-1, the reduced form of lipoxygenase contains an iron(II) ion ligated with six ligands including three imidazoles, one carboxylato, one asparagine and one water molecule, while in 15-rabbit lipoxygenase, it contains an

iron(II) ion with four imidazoles, one carboxylato and another vacant site capable of accommodating ligand like glycerol (Scheme 18).[31]

As elucidated in oxygen rebound mechanism, the $Fe^{IV}=O^{+\bullet}$ form of the compound I in P450 enzymes abstracts a hydrogen atom from substrate to form a Fe^{IV}-OH moiety which will *in situ* rebind the OH group back to the substrate radical to generate alcohol product. However, such kind of Fe^{IV}-OH form of compound II was not directly observed in P450 enzymes, and the compound IIs in both P450 enzymes and peroxidases were generally represented in a $Fe^{IV}=O$ form. In 2004, Green reported that in chloroperoxidase (CPO), the compound II is in a Fe^{IV}-OH form rather than the believed $Fe^{IV}=O$ form, since the X-ray absorption spectroscopy disclosed that the Fe-O bond length (1.82 Å) in the compound II of CPO is much longer than those in other peroxidases (1.64 Å). Meanwhile, the resonance Raman signal from $Fe^{IV}=O$ stretching in the compound II is absent, which leads to the conclusion that the active form of iron in CPO-I is $Fe^{IV}=O$ while it is Fe^{IV}–OH in CPO-II.[7] Even in xanthine oxidases, which catalyze hydroxylation of the C–H bond at the 8-position of hypoxanthine, it has both $Mo^{VI}=O$ and Mo^{VI}-OH functional groups in its active site, however, the identified active functional group is the Mo^{VI}-OH rather than the corresponding $Mo^{VI}=O$.[32] These discoveries have invoked the interests to investigate the oxidative reactivity of the active M^{n+}-OH, and its comparison with the corresponding $M^{n+}=O$ moieties.

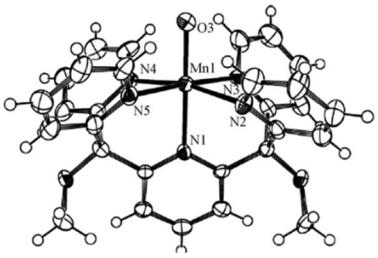

Scheme 19 The crystal structure of $[Mn^{III}(PY5)(OH)]^{2+}$. Reprinted with permission from ref. 34. Copyright 2005 American Chemical Society.

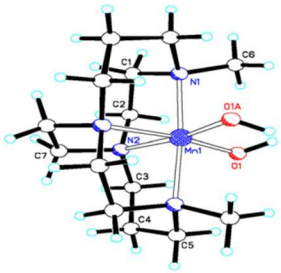

Scheme 20 Crystal structure of $[Mn(Me_2EBC)(OH)_2]^{2+}$. Reprinted with permission from ref. 35. Copyright 2006 American Chemical Society.

3.1 Hydrogen abstraction reactivity of the active metal hydroxo moiety in synthetic models

Stack and co-workers synthesized both iron(III) and manganese(III) models of lipoxygenases including $[Fe^{III}(PY5)(OH)]^{2+}$ and $[Mn^{III}(PY5)(OH)]^{2+}$ (PY5: 2,6-bis-(bis(2-pyridyl)methoxymethane)pyridine)) (Scheme 19), and confirmed that both of them are capable of hydrogen abstraction from the activated C–H bonds. Using the method introduced by Bordwell and Mayer,[2] they found that the hydrogen abstraction abilities of the Fe^{III}-OH and Mn^{III}-OH moieties in their models are limited to 80 and 82 kcal/mol, respectively, indicating that they are only capable of abstracting hydrogen from activated C–H bonds, like those in 1,4-pentadiene subunit-containing fatty acids by lipoxygenases.[33, 34] However, the experimental tests with selected substrates having known C-H bond dissociation energy (BDE) reveal that both of Fe^{III}-OH and Mn^{III}-OH in models are capable of abstracting hydrogen atom from ethylbenzene or toluene which has a BDE_{C-H} value of 85 or 88 kcal/mol, while the H/D KIEs still confirm that the reaction proceed by hydrogen atom transfer.

Busch and Yin synthesized and well-characterized a monomeric manganese(IV) complex (Scheme 20) with two hydroxide ligands, $[Mn(Me_2EBC)(OH)_2]^{2+}$ (Me_2EBC: 4,11-dimethyl-1,4,8,11-tetraazabicyclo[6.6.2]hexadecane).[35] The existence of monomer for this manganese(IV) complex has been attributed to the presence of methyl groups on the two non-bridging amines which prohibits the formation of oxo bridged dimmers or oligomers. This manganese(IV) complex demonstrates a gentle oxidizing power with a redox potential of +0.756 V (*vs* SHE) for the Mn^{IV}/Mn^{III} couple; accordingly, it is relatively stable in aqueous solution. The determined accurate pK_a value for the manganese(IV) complex is 6.86, which corresponds to deprotonation of $[Mn(Me_2EBC)(OH)_2]^{2+}$ to form $[Mn(Me_2EBC)(O)(OH)]^{+}$, a second approximate pK_a at 10 is related to loss of last proton to generate neutral $Mn(Me_2EBC)(O)_2$, and a more approximate pK_a at 2~3 represents adding one proton to $[Mn(Me_2EBC)(OH)_2]^{2+}$ to form $[Mn(Me_2EBC)(OH)(OH_2)]^{3+}$. Because of its relative stability in aqueous solution with three well-separated and well-controllable pK_a values (2~3, 6.86 and 10), this manganese(IV) complexes provides a unique chance to compare the reactivity of the active M^{n+}-OH with its corresponding $M^{n+}=O$ moiety in oxidations (*via infra*).

In addition to above monomeric manganese(IV) complex, another significant monomeric manganese(IV) complex having two hydroxide ligands, $[Mn(Pytacn)(OH)_2](CF_3SO_3)_2$ was synthesized and well characterized by Costas and co-workers (Scheme 21).[36] Similar to $[Mn(Me_2EBC)(OH)_2]^{2+}$, two hydroxide ligands of this manganese(IV) complex are in a *cis* arrangement relative to each other, and the N-methyl groups with the pyridine ring provides steric isolation of the metal center, which is the key feature to prevent the formation of oligomer species. The pK_a value of this complex is 7.1, corresponding to release one proton to form $[Mn(Pytacn)(O)(OH)]^{+}$, which is similar with that of $[Mn(Me_2EBC)(OH)_2]^{2+}$ (6.86). The hydrogen abstraction by $[Mn(Pytacn)(OH)_2]^{2+}$ showed a first-order dependence both in substrate and manganese(IV) concentrations, and the large KIE values for xanthene (8.0) and 1,4-cyclohexadiene (6.6) suggest

the reaction proceeds by hydrogen atom transfer pathway. In particular, the $[Mn(Pytacn)(O)(OH)]^+$ demonstrates a saturation kinetic behaviour on substrate, indicating the formation of a C-H substrate/H-abstractor encounter complex.

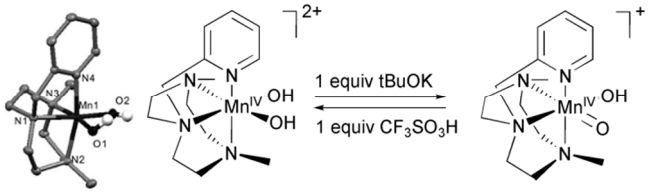

Scheme 21 The thermal ellipsoid diagram (left) of $[Mn(Pytacn)(OH)_2]^{2+}$ and its titration from $Mn^{IV}(OH)_2^{2+}$ to $Mn^{IV}O(OH)^+$. Reprinted with permission from ref. 36. Copyright 2011 Wiley-VCH.

Copper-oxygen moieties are also implicated as the intermediates in a wide range of enzymatic and chemical oxidations, and great efforts have been paid to isolate and characterize these reactive intermediates. Tolman and co-workers synthesized a LCu^{III}-OH complex generated by one electron oxidation of corresponding LCu^{II}-OH (L: N,N'-bis(2,6-diisopropylephenyl)-2,6- pyridinedicarboxamide).[37] The synthetic Cu^{III}-OH complex can react with dihydroanthracene (DHA) to yield dominant anthracene product with the reduced Cu(II) complex (Scheme 22), and the kinetic studies revealed that the reaction occurs via hydrogen atom transfer pathway with a very large KIE value (44 at 203 K).

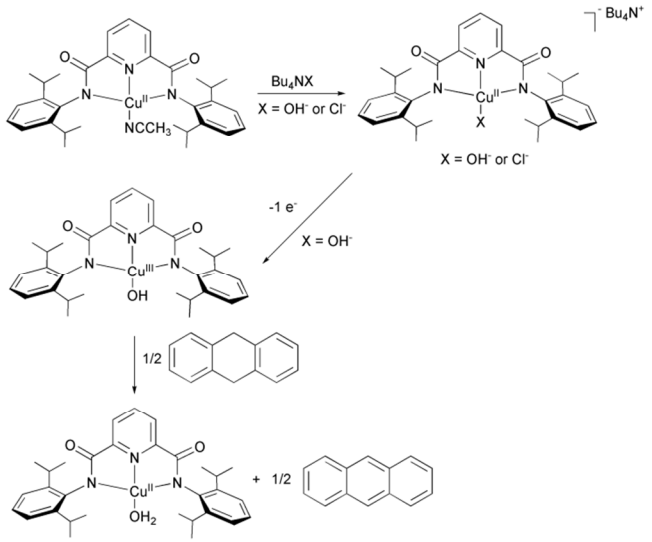

Scheme 22 Cu^{III}-OH complex generated by one electron oxidation of corresponding Cu^{II}-OH complex and hydrogen abstraction reaction with dihydroanthracene. Reprinted with permission from ref. 37. Copyright 2011 American Chemical Society.

3.2 The reactivity similarities and differences of the metal hydroxo and oxo moieties in hydrogen abstraction

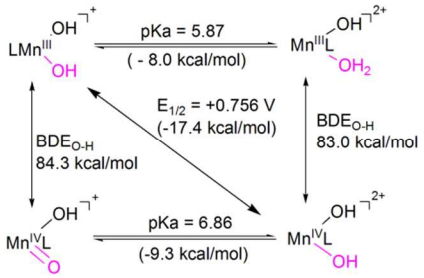

Scheme 23 Thermodynamic evaluation of hydrogen abstraction capability of the Mn^{IV}–OH and Mn^{IV}=O groups in $Mn^{IV}(Me_2EBC)$ complex. Reprinted with permission from ref. 38. Copyright 2007 American Chemical Society.

Although the reported synthetic models to demonstrate the oxidizing power of the M^{n+}-OH moiety are still very limited when compared with the corresponding M^{n+}=O moieties, the increasing information has clearly revealed that the M^{n+}-OH moiety may also play significant roles in versatile biological and chemical oxidations. The immediate issue is that "*what are the reactivity differences and similarities between M^{n+}-OH and M^{n+}=O moieties in oxidation?*" Using the equation introduced by Bordwell and Mayer, Busch and Yin found that the hydrogen abstraction abilities of the Mn^{IV}=O group in $[Mn(Me_2EBC)(O)(OH)]^+$ and the Mn^{IV}–OH group in $[Mn(Me_2EBC)(OH)_2]^{2+}$ are surprisingly similar (84.3 *vs* 83.0 kcal/mol) (Scheme 23), and independent experimental tests further confirmed their similar hydrogen abstraction abilities, that is, both are limited to 82 kcal/mol.[38] They also demonstrate a very similar KIE in hydrogen abstraction from DHA (3.27 for Mn^{IV}–OH *vs* 3.78 for Mn^{IV}=O), indicating both of them have hydrogen atom transfer as the rate determining step. However, the authors also observed that the Mn^{IV}=O moiety can abstract hydrogen atom about 40 times faster than the corresponding Mn^{IV}-OH (Table 1).[39]

Table 1 The second order rate constants for hydrogen abstraction from substrates with $[Mn^{IV}(Me_2EBC)(OH)_2]^{2+}$ and $Mn^{IV}(Me_2EBC)(O)_2$.

substrate	BDE_{CH} (kcal/mol)	k_{2OH} at pH 4.0 (M^{-1} s^{-1})	k_{2OXO} at pH 13.4 (M^{-1} s^{-1})	k_{2OXO}/k_{2OH}
xanthene	75.5	0.00107	0.048	44.9
1,4-cyclohexadiene	76	3.64×10^{-4}	0.0159	43.7
9,10-dihydroxyanthracene	78	3.52×10^{-4}	0.01496	42.5
fluorene	80	$\sim 2.5 \times 10^{-4}$	0.00912	~36.5

Conditions: solvent, acetone/water (ratio 4:1), initial concentrations of substrate, 40 mM, and manganese(IV) complex, 4 mM, at 288 K.

Similar hydrogen abstraction reactivity of Mn^{IV}-OH with Mn^{IV}=O moiety was also observed by Fujii and co-workers.[40] In their Mn(Salen) model (Scheme 24), Mn^{IV}=O moiety reacts readily with 4-NC-2,6-*tert*-$Bu_2C_6H_2OH$ which has a BDE_{OH} value of 84.2 kcal/mol at 203 K, while the corresponding Mn^{IV}-OH is only capable of abstracting hydrogen from 4-CH_3CO-2,6-*tert*-$Bu_2C_6H_2OH$ with BDE_{OH} value of 83.1 $kcal/mol^{-1}$, and its rate is significantly slower than that of Mn^{IV}=O, very similar to those in $[Mn(Me_2EBC)(OH)_2]^{2+}$ model. A significant kinetic isotope effect (k_H/k_D = 5.3 and 9.5 respectively) was also observed for reactions of (Salen)Mn^{IV}=O and (Salen)Mn^{IV}–OH

with 2,6-di-*tert*-butylphenol-d, suggesting that the rate determining step involves O-H bond cleavage. However, the Mn^{IV}-OH moiety in Mn(Salen) model is incapable of hydrogen abstraction from C-H bond, which makes no comparison with the corresponding Mn^{IV}=O moiety in C-H bond cleavage.

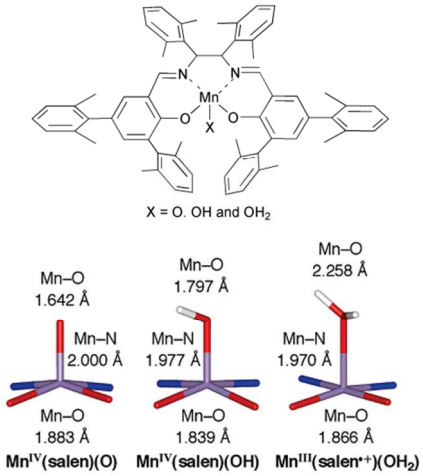

Scheme 24 Molecular structures of Mn(Salen) complexes with the calculated Mn-O bond length. Reprinted with permission from ref. 40. Copyright 2008 American Chemical Society.

Que and co-workers compared the hydrogen abstraction reactivity of Fe^{IV}=O and Fe^{IV}-OH moieties in [Fe^{IV}(β-BPMCN)] model (BPMCN: N,N'-bis(2-pyridylmethyl)-N,N'-dimethyltrans-1,2-diaminocyclohexane).[41] It was found that the activity of iron(IV) moieties is much higher than that of manganese(IV) moieties. For example, the second order rate constant for hydrogen abstraction from 1,4-cyclohexadiene by Fe^{IV}-OH is $4x10^{-4}$ $M^{-1}s^{-1}$ at 203 K, which is comparable to that ($3.64x10^{-4}$ $M^{-1}s^{-1}$) of Mn^{IV}-OH in $[Mn(Me_2EBC)(OH)_2]^{2+}$ at 288 K. Significantly, the Fe^{IV}=O moiety also demonstrated much faster rate than the corresponding Fe^{IV}-OH moiety (generally above 100-fold).

Table 2 The kinetic parameters for hydrogen abstraction from DHA-h_4 and DHA-d_4 by Mn^{IV}–OH and Mn^{IV}=O in $Mn^{IV}(Me_2EBC)$ complexes.[42]

Mn(IV) moiety	Mn^{IV}-OH	Mn^{IV}=O
E_H (kcal/mol)	15.6 ± 0.5	14.3 ± 0.6
E_D (kcal/mol)	21.7 ± 0.6	20.3 ± 0.5
A_H (s^{-1})	9.3 x 10^6	7.6 x 10^7
A_D (s^{-1})	6.5 x 10^{10}	7.3 x 10^{11}
$\Delta H_H^{\neq}$(kcal/mol)	15.2 ± 0.6	13.7 ± 0.6
$\Delta S_H^{\neq}$(cal.mol^{-1}.K^{-1})	-27.9 ± 2.0	-24.5 ± 2.2
$\Delta H_D^{\neq}$(kcal/mol)	21.1 ± 0.6	19.7 ± 0.7
$\Delta S_D^{\neq}$(cal.mol^{-1}.K^{-1})	-11.1 ± 1.9	-6.3 ± 2.3
E_D-E_H	6.1	6.0
A_H/A_D	1.43 x 10^{-4}	1.1 x 10^{-4}
$\Delta\Delta H^{\neq}_{H/D}$	5.9	6.0
$\Delta\Delta S^{\neq}_{H/D}$	-16.8	-18.2
a (Å)	0.60	0.58
Q_t	4.50	4.36

The detailed kinetics of hydrogen atom abstraction by Mn^{IV}=O and Mn^{IV}–OH moieties was further investigated by Yin and co-workers with $[Mn(Me_2EBC)(OH)_2]^{2+}$ model.[42] A list of kinetic data including the activation energy (E) and prefactor (A) according to the Arrhenius equation, activation enthalpy ($\Delta H^{\neq}$) and activation entropy ($\Delta S^{\neq}$) according to the Eyring equation, as well as barrier half-width (*a*) and the tunnelling correction (Q_t) were evaluated for hydrogen abstraction from DHA-h_4 and DHA-d_4 by the Mn^{IV}=O and Mn^{IV}–OH moieties independently. As listed in Table 2, their kinetic parameter differences in H/D abstraction ($\Delta\Delta H^{\neq}_{H/D}$, $\Delta\Delta S^{\neq}_{H/D}$, A_H/A_D, *a*, Q_t) are unexpectedly similar, implicating that the reactive characters of the Mn^{IV}=O and Mn^{IV}–OH moieties in the transition states of hydrogen abstraction are possibly very similar except their rate differences due to the different activation energy barriers. However, in nature, the redox enzyme's choice on M^{n+}=O and M^{n+}-OH moieties is highly specific, and the different choices are apparently not due to their similar characters in hydrogen abstraction with different rates. Thus, the critical factors dominating the redox enzymes to select a M^{n+}=O or M^{n+}-OH functional group to serve as the active species is possibly not related with their reactive similarities but with other issues.

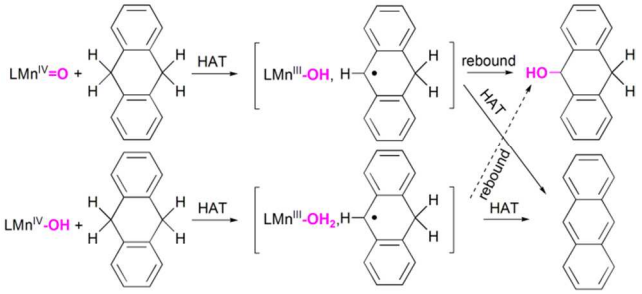

Scheme 25 Distinct mechanisms in oxidation of 9,10-dihydroanthracene by Mn^{IV}=O and Mn^{IV}-OH in $Mn^{IV}(Me_2EBC)$ complex. Reprinted with permission from ref. 43. Copyright 2011 Wiley-VCH.

After analysing the product distributions in independent hydrogen abstraction from DHA by Mn^{IV}-OH and Mn^{IV}=O in $Mn^{IV}(Me_2EBC)(OH)_2^{2+}$ model, Yin and co-workers disclosed that, hydrogen abstraction by Mn^{IV}-OH can only produce anthracene, whereas the Mn^{IV}=O moiety yields anthracene and anthraquinone. Obviously, anthracene is a desaturation product, while anthraquinone is a hydroxylation product by further oxidation of 9-hydroxy-9,10-dihydroanthracene. As stated in section 2.1, the M^{n+}=O moiety is capable of serving hydroxylation through oxygen rebound mechanism and desaturation by further abstracting second hydrogen atom from nearby carbon site (see Scheme 2). Here, it has been found that the Mn^{IV}-OH is incapable of performing hydroxylation reaction. Clearly, the reactivity properties of the Mn^{IV}-OH and Mn^{IV}=O moieties are different after the first hydrogen abstraction. For the Mn^{IV}-OH, after hydrogen abstraction, the reduced Mn^{III}-OH_2 cannot play oxygen rebound mechanism, since it has no OH group to rebind over to the substrate radical to generate the hydroxylation product (Scheme 25). In contrast, the reduced Mn^{III}-OH from Mn^{IV}=O is capable of rebounding

the OH group to the substrate radical to form the oxygenation product.[43] The distinct reactivity differences of the M^{n+}=O and M^{n+}-OH moieties after hydrogen abstraction are critical for understanding the origins of redox metalloenzymes to select them in serving the key intermediate in a specific oxidation event (*via infra*).

3.3 The oxygenation and electron transfer differences of the metal hydroxo and oxo moieties.

Compared with relatively extensive studies on hydrogen abstraction, the reports on oxygen transfer and electron transfer reactivity of the M^{n+}-OH moiety are very limited. Yin and co-workers even investigated the oxygenation of triarylphosphines by $Mn^{IV}(Me_2EBC)(OH)_2^{2+}$ model. The substituent effects in Hammett plot revealed that oxygenation by the $Mn^{IV}(Me_2EBC)$ complex having Mn^{IV}=O group proceeds by concerted oxygen transfer which is insensitive to the substituents on triphenylphosphine (ρ = -0.08),[44] while it proceeds by electron transfer for the $Mn^{IV}(Me_2EBC)$ complex with Mn^{IV}-OH group having ρ value of -0.697 in Hammett plot (Fig. 2), which is very similar to that of triphenylphosphine oxygenation by Cr^{V}=O (see scheme 15). Particularly, the solvent kinetic isotope effect using ^{18}O-water disclosed an inverse KIE value (k_{H2O}/k_{D2O} = 0.578 at 288 K), indicating that protonation of $Mn^{IV}(Me_2EBC)(OH)_2^{2+}$ to form $Mn^{IV}(Me_2EBC)(OH)(OH_2)^{3+}$ is prior to electron transfer. That is, it is $Mn^{IV}(Me_2EBC)(OH)(OH_2)^{3+}$, rather than $Mn^{IV}(Me_2EBC)(OH)_2^{2+}$, responsible for triphenylphosphine oxygenation. It is worth to note that both $Mn^{IV}(Me_2EBC)(OH)_2^{2+}$ and $Mn^{IV}(Me_2EBC)(OH)(OH_2)^{3+}$ have the Mn^{IV}-OH functional group, and the viable difference between them is their different positive net charge, that is 2+ in $Mn^{IV}(Me_2EBC)(OH)_2^{2+}$ and 3+ $Mn^{IV}(Me_2EBC)(OH)(OH_2)^{3+}$.

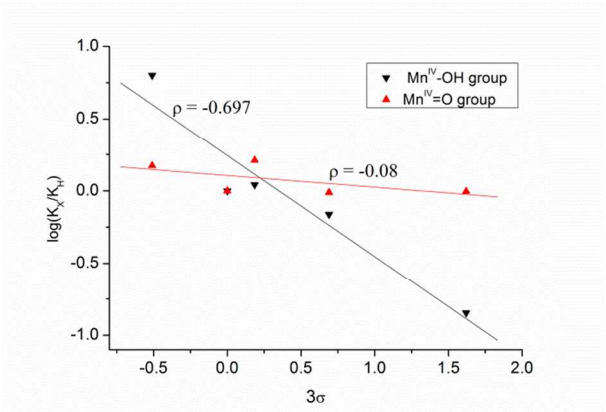

Fig. 2 Hammett plot for the oxygenation of triarylphosphanes by Mn^{IV}-OH and Mn^{IV}=O moieties in acetone/water (4:1) at 293 K. Reprinted with permission from ref. 44. Copyright 2009 Wiley-VCH.

Following this study, Yin and co-worker further investigated the influence of the net charge on the reactivity of the manganese(IV) species in $Mn^{IV}(Me_2EBC)(OH)_2^{2+}$ model.[45] As disclosed earlier, this manganese(IV) complex has three feasibly controllable pK_a values, one accurate at 6.86, representing the releasing of first proton to form $Mn^{IV}(Me_2EBC)(O)(OH)^{+}$, one approximate at 10 corresponding to release last proton to form neutral $Mn^{IV}(Me_2EBC)(O)_2$, and another more approximate at 2~3 representing adding one proton to form $Mn^{IV}(Me_2EBC)(OH)(OH_2)^{3+}$. Thereof, $Mn^{IV}(Me_2EBC)(OH)(OH_2)^{3+}$ having 3+ net charge may dominate at pH 1.5, $Mn^{IV}(Me_2EBC)(OH)_2^{2+}$ having 2+ net charge dominates at pH 4.0, and $Mn^{IV}(Me_2EBC)(O)_2$ having zero charge dominates at pH 13.4, thus providing a unique platform to investigate the influence the net charge on the reactivity of an active metal ion species (Scheme 26).

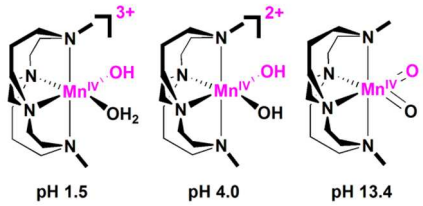

Scheme 26 The net charge and form of the manganese(IV) species under different pH conditions in $Mn^{IV}(Me_2EBC)(OH)_2^{2+}$ complex. Reprinted with permission from ref. 45. Copyright 2012 American Chemical Society.

Table 3 Rate differences of electron transfer from $(4\text{-MeOPh})_3P$ by the manganese(IV) species from $Mn^{IV}(Me_2EBC)$ complex having different charge.[45]

Temp. (K)	k_2 at pH 1.5 (M^{-1} s^{-1})	k_2 at pH 4.0 (M^{-1} s^{-1})	$k_{2,pH\ 1.5}/k_{2,pH\ 4.0}$
273	0.470±0.020	0.022±0.002	21.4
283	0.806±0.030	0.045±0.001	17.9
293	1.70±0.059	0.174±0.002	9.8

Conditions: acetone/water (ratio 4:1), initial concentration of manganese(IV) 1 mM.

Using tris(4-methoxyphenyl)phosphine as substrate, Yin and co-workers found that the solvent kinetic isotope effect is normal (k_{H2O}/k_{D2O} = 1.55 at 293 K) in oxygenation by $Mn^{IV}(Me_2EBC)(OH)_2^{2+}$, indicating that its protonation is not essential prior to oxygenation. The kinetics of tris(4-methoxyphenyl)phosphine oxygenation revealed that $Mn^{IV}(Me_2EBC)(OH)(OH_2)^{3+}$ having 3+ net charge demonstrates above 10-fold faster rate than does the $Mn^{IV}(Me_2EBC)(OH)_2^{2+}$ having 2+ net charge (Table 3), and the Hammett plot still revealed that the oxygenation proceeds by electron transfer. To compare the electron transfer between $Mn^{IV}(Me_2EBC)(OH)_2^{2+}$ having 2+ net charge with neutral $Mn^{IV}(Me_2EBC)(O)_2$, Yin and co-workers selected ABTS as substrate which is a typical electron transfer reagent (see Scheme 12 above, note: triarylphosphine oxygenation by $Mn^{IV}(Me_2EBC)(O)_2$ proceeds by concerted oxygen transfer, thus it is not a suitable substrate to investigate electron transfer by Mn^{IV}=O). It was found that electron transfer between $Mn^{IV}(Me_2EBC)(OH)_2^{2+}$ and ABTS can be achieved in minutes, while it does not happen for $Mn^{IV}(Me_2EBC)(O)_2$, supporting that $Mn^{IV}(Me_2EBC)(OH)_2^{2+}$ having 2+ net charge have much more powerful electron transfer ability than the neutral $Mn^{IV}(Me_2EBC)(O)_2$ (Fig. 3). Different electron transfer capabilities of the manganese(IV) species having 3+, 2+ and

zero net charge are also consistent with their different potentials which are +0.54, +0.46 and +0.10 (*vs* SCE), respectively.

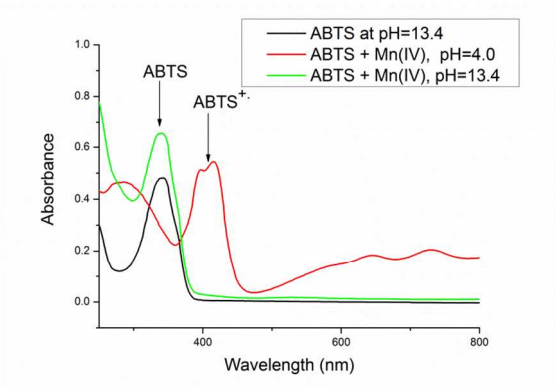

Fig. 3 The UV-Vis spectra of electron transfer tests from ABTS by manganese(IV) complex in aqueous solution (modified from ref. 43).

Although the M^{n+}=O moiety generally demonstrates much faster hydrogen abstraction rate than the corresponding M^{n+}-OH moiety as stated earlier, for the identical Mn^{IV}-OH moieties in one model, for example, $Mn^{IV}(Me_2EBC)(OH)(OH_2)^{3+}$ *vs* $Mn^{IV}(Me_2EBC)(OH)_2{}^{2+}$, increasing one unit of positive net charge does not affect its hydrogen abstraction rate (Table 4),[45] and the hydrogen abstraction capability of the Mn^{IV}-OH in $Mn^{IV}(Me_2EBC)(OH)(OH_2)^{3+}$ is also limited to 82 kcal/mol as well as Mn^{IV}-OH in $Mn^{IV}(Me_2EBC)(OH)_2{}^{2+}$ and Mn^{IV}=O in $Mn^{IV}(Me_2EBC)(O)_2$, even though their pK_as and redox potentials have changed with the changes of the net charge. The comparable hydrogen abstraction capability of the M^{n+}-OH with the corresponding M^{n+}=O moiety has been assigned to the compensation effect between pK_a and potential which will be discussed in next section.

Table 4 Rate differences of hydrogen abstraction from 1,4-cyclohexadiene by manganese(IV) species from $Mn^{IV}(Me_2EBC)$ complex having different charge.[45]

Temp. (K)	k_2 at pH 1.5 (M^{-1} s^{-1})	k_2 at pH 4.0 (M^{-1} s^{-1})	$k_{2,pH\ 1.5}/k_{2,pH\ 4.0}$
293	$(9.09\pm0.07)\times10^{-4}$	$(8.68\pm0.08)\times10^{-4}$	1.05
303	$(1.73\pm0.08)\times10^{-3}$	$(1.52\pm0.01)\times10^{-3}$	1.14
313	$(2.86\pm0.09)\times10^{-3}$	$(2.90\pm0.09)\times10^{-3}$	0.99

Conditions: acetone/water (ratio 4:1), initial concentration of manganese(IV) 1 mM.

4 The relationship of the physicochemical properties of a redox metal ion with its reactivity and its implications in oxidations

As stated earlier, the viable difference between M^{n+}=O and M^{n+}-OH moieties is the protonation state of the metal-oxygen bond. With protonating of the M^{n+}=O functional group, the metal-oxygen bond order changes from double to single bond, which leads to the net charge, redox potential and the oxidative reactivity changes of the central metal ion. Clarifying how the reactivity of an redox metal ion changes with the changes of these physicochemical properties would apparently benefit the prediction of its reactivity under a certain chemical environment, the elucidation of unveiled enzymatic mechanisms, the explanation of elusive oxidation phenomena, and the design of selective redox catalyst. However, the available models to compare the reactivity of the M^{n+}=O with its corresponding M^{n+}-OH moiety under identical coordination environment are very limited.

Table 5 The thermodynamic parameters and oxidative activity of the manganese(IV) species from the $Mn^{IV}(Me_2EBC)$ complex.[45]

Mn^{IV} moiety	$[LMn^{IV}\text{-}OH]^{3+}$	$[LMn^{IV}\text{-}OH]^{2+}$	$[LMn^{IV}=O]$
Net charge	3+	2+	0
$E_{1/2}$ (V) *vs* SCE	+0.54	+0.46	+0.10
pK_a of the corresponding Mn^{III} complex	~1.6	5.87	-
$BDFE_{O\text{-}H}$ (kcal/mol)	77.8	81.9	-
Electron transfer rate	$[LMn^{IV}\text{-}OH]^{3+}$ >	$[LMn^{IV}\text{-}OH]^{2+}$ >>	$[LMn^{IV}=O]$
Hydrogen abstraction rate	$[LMn^{IV}\text{-}OH]^{3+}$ ~	$[LMn^{IV}\text{-}OH]^{2+}$ <<	$[LMn^{IV}=O]$

4.1 The relationship of the physicochemical properties of a redox metal ion with its reactivity

Due to the stability and/or oxidizing capability of these models, until now, there has been only one model, that is, $Mn^{IV}(Me_2EBC)(OH)_2{}^{2+}$, achieving the extensive studies on the reactivity of the M^{n+}=O and its corresponding M^{n+}-OH moiety. After comparing the electron transfer, hydrogen abstraction and oxygen transfer reactivity of the Mn^{IV}-OH and Mn^{IV}=O in $Mn^{IV}(Me_2EBC)(OH)_2{}^{2+}$ model, Yin and co-workers summarized the thermodynamic parameters and the oxidative properties of the manganese(IV) species in $Mn^{IV}(Me_2EBC)$ complex as shown in Table 5.[45] One may see that three forms of manganese(IV) species may occur in this manganese(IV) model because of different protonation states, including neutral Mn^{IV}=O, Mn^{IV}-OH having 2+ net charge, and Mn^{IV}-OH having 3+ net charge. With the net charge increasing from zero to 2+, then 3+, the redox potential of Mn^{III}/Mn^{IV} couple increases from +0.10, to +0.46, then to +0.54 V (*vs* SCE). The pK_a of the corresponding reduced Mn(III) complex changes inversely. For example, it is 5.87 for the Mn^{IV}-OH having 2+ net charge, while it is 1.6 for the Mn^{IV}-OH having 3+ net charge. Although the pK_a value of the reduced Mn(III) species from the neutral Mn^{IV}=O is unknown, it should be highly basic to provide the driving force for the hydrogen abstraction by the Mn^{IV}=O in neutral $Mn^{IV}(Me_2EBC)(O)_2$ (Experimentally, it can abstract hydrogen atom with BDE value below 82 kcal/mol). According to the equation described by Mayer, the thermodynamic driving force of a redox metal ion can be evaluated with its redox potential and the pK_a value of its corresponding reduced metal ion (Eq. 1).[2] As demonstrated in Table 5, the trend of potential is contrast to that of pK_a, indicating that there exists compensation effect between them. That is, under the certain coordination environment, the thermodynamic driving force of a redox metal ion in its hydrogen abstraction would not change seriously in different conditions, because in the case of its

potential increases, its pK_a would decrease simultaneously, or vice versa.

Later, similar compensation effect was also described by Kovacs in their Mn^{III}-OR (R = $^{p}NO_2Ph$, Ph, Me, H) complexes having SMe_2N_4(tren) ligand (Fig. 4).[46] In their studies, due to the very low cathodic peak potentials ($E_{p,c}$) of these Mn(III) complexes (Table 6), one would not expect they are capable of abstracting hydrogen from TEMPOH, and particularly, based on their $E_{p,c}$, one may predict that the Mn(III) complex having phenoxide ligand could have better oxidizing power than the corresponding methoxide or hydroxide complex. However, this is contrast to the observed reactivity in which the methoxide and hydroxide complexes, but not phenoxide complexes, demonstrate oxidizing capability to TEMPOH. To facilitate the hydrogen abstraction from TEMPOH in CH_3CN by the hydroxide complex which has a redox potential of -0.6 V (*vs* Cp_2Fc^+/ Cp_2Fc), the pK_a value of the reduced Mn^{II}-OH_2 should be lower than 18.5 according to Eq. 1, and the estimated value by Kovacs is 21.4. Kovacs further calculated the required pK_a values of other Mn^{III}-OR complexes for hydrogen abstraction from TEMPOH in CH_3CN. To achieve the identical hydrogen abstraction ability from TEMPOH, the required pK_a of the reduced metal ion are apparently contrary to the corresponding potential.

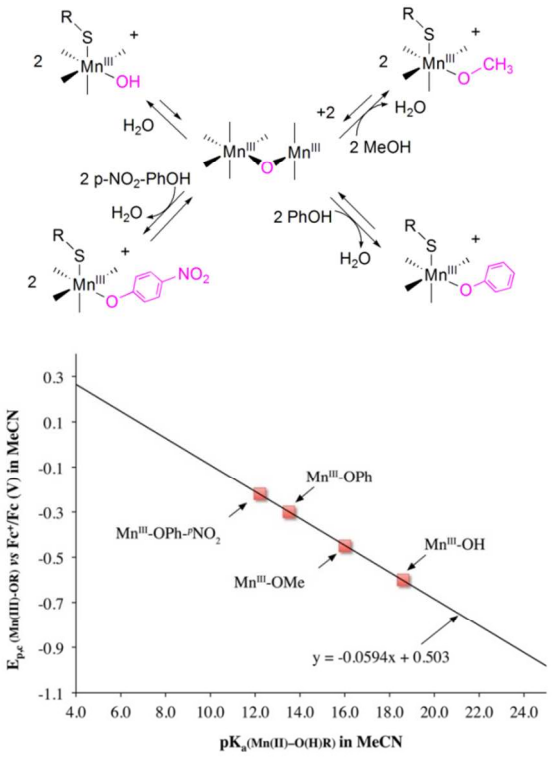

Fig. 4 Conversion of oxo-bridged manganese complex to monomeric hydroxide-ligated complexes Mn^{III}-OR (R = $^{p}NO_2Ph$, Ph, Me, H) and the required pK_a of the reduced metal ion as a function to the corresponding redox potential to achieve the identical hydrogen abstraction ability from TEMPOH in MeCN. Reprinted with permission from ref. 46. Copyright 2013 American Chemical Society.

Table 6 Redox properties and proton affinity of $Mn^{III/II}OR$ (R = $^{p}NO_2Ph$, Ph, Me, H) compounds in MeCN.[46]

Mn(IV) moiety	$E_{p,c}$ (mV *vs* $Fc^{+/0}$) in MeCN	Estimated pKa of $Mn^{II}O(H)R$ in MeCN
$MnOPh^{p}NO_2$	-220	<12.2
MnOPh	-300	<13.5
MnOMe	-450	≥16.2
MnOH	-600	21.2

In the method introduced by Bordwell and Mayer, the thermodynamic driving force in hydrogen abstraction of a redox metal ion is determined by both of its potential and related pK_a value of its reduced form.[2] However, the compensation effect between potential and pK_a has further defined its oxidizing capability to a comparable level as observed by Yin and Kovacs. That is, having the similar coordination environment, one may not expect to substantially improve the oxidizing power of a redox metal ion by increasing its potential while remaining the pK_a value of its reduced form unchanged, or vice versa. This compensation effect may help to understand why the metalloenzymes can metabolize those robust substrates but do not damage the protein itself. In P450 enzymes, the highly basic character of the ferryl oxo has largely compensated its relatively low potential which is required to avoid the protein damage by one electron oxidation. Such a phenomenon has also been observed in Goldberg's synthetic $[Mn^{V}(TBP_8Cz)(O)]$ complex (TBP_8Cz : octakis(*p-tert*-butylphenyl)corrolazinato^{3-}).[47] Although it only has a potential of +0.24 V (*vs* SHE), it can cleavage the C-H or O-H bond of a variety of substrate. To facilitate its high oxidizing ability, the estimated pK_a value would be as high as 15 in acetonitrile. In another example, Borovik reported a $[Mn^{III}H_3buea(O)]^{2-}$ complex which has the potential of as low as -1.3 V, however, it is capable of abstracting hydrogen from 9,10-dihydroanthracene (BDE_{CH} 78 kcal/mol), because its measured pK_a value is as high as 28.3 in DMSO.[48]

Also as demonstrated in Table 3, increasing the net charge of the Mn(IV) species through protonation would greatly accelerates its electron transfer rate, because its redox potential increases as well. Similar accelerate effect was also observed by Fukuzumi and Nam. Originally, $[(N4Py)Fe^{IV}(O)]^{2+}$ is incapable of oxidize $[Ru^{II}(Clphen)_3]^{2+}$ because its potential (E_{red} = +0.51 V *vs* SCE) is lower than that of $[Ru^{II}(Clphen)_3]^{2+}$ (E_{ox} = +1.36 V *vs* SCE).[49] However, in the presence of $HClO_4$, the electron transfer from $[Ru^{II}(Clphen)_3]^{2+}$ to $[(N4Py)Fe^{IV}(O)]^{2+}$ proceeds efficiently. As disclosed by the authors, the presence of $HClO_4$ may protonate the $[(N4Py)Fe^{IV}(O)]^{2+}$ to generate the $[(N4Py)Fe^{IV}(OH)]^{3+}$ species, thus shifts it redox potential from +0.51 V to +1.43 V. Furthermore, not only accelerating electron transfer rate, protonation of $[(N4Py)Fe^{IV}(O)]^{2+}$ by $HClO_4$ can also accelerate its sulfide oxygenation by 1000-fold.

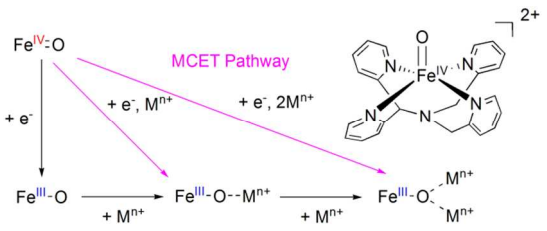

Scheme 27 Lewis acid accelerated electron transfer by $[(N4Py)Fe^{IV}(O)]^{2+}$. Reprinted with permission from ref. 50. Copyright 2011 American Chemical Society.

As well as Brönsted acid promoted electron transfer, Fukuzumi and Nam found that the non-redox metal ions as Lewis acid may also greatly accelerate the active M^{n+}=O mediated electron transfer. For example, the authors found that, in electron transfer from $[Fe(bpy)_3]^{2+}$ to $[(N4Py)Fe^{IV}(O)]^{2+}$, adding Sc^{3+} would accelerate rate up to 10^8-fold, the redox potential of $[(N4Py)Fe^{IV}(O)]^{2+}$ can be shifted positively by 0.84 V in the presence of 0.2 M Sc^{3+} ion (Scheme 27).[50] Notably, in sulfide oxygenation, adding Sc^{3+} can shift the oxygenation mechanism of $[(N4Py)Fe^{IV}(O)]^{2+}$ from direct oxygen transfer to electron transfer, and the rate is accelerated as much as 100-fold.[51] These works have been reviewed by Fukuzumi elsewhere[1]. In addition to the Brönsted acid and Lewis acid promoting M^{n+}=O mediated stoichiometric electron transfer and oxygenation, Yin and co-workers found that Lewis acid can also accelerate the redox metal ions mediated stoichiometric and catalytic oxidations which has a hydroxo rather than oxo functional group.[52] In triphenylphosphine oxygenation by $Mn^{IV}(Me_2EBC)(OH)^{2+}$, they found that the rate can be substantially accelerated in the presence of non-redox metal ions like Al^{3+}, and the rate enhancements are highly Lewis acid strength dependent (Fig. 5). In catalytic sulfoxidation with the $Mn^{II}(Me_2EBC)Cl_2$ catalyst, similar Lewis accelerated oxygenations were also observed, and the acceleration effect is also Lewis acid strength dependent (Fig. 6). Further characterizations of $Mn^{IV}(Me_2EBC)(OH)^{2+}$ complex in the presence of Lewis acid revealed that Lewis acid can bind to the complex through the Mn^{IV}-O-LA^{m+} bridge (LA: Lewis acid), which leads to the positive shift of the redox potential of the Mn^{IV}/Mn^{III} couple.

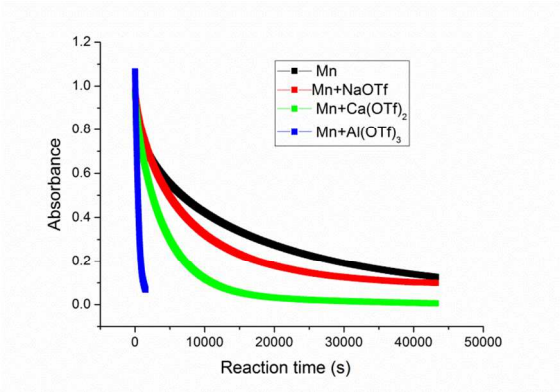

Fig. 5 Oxygenation kinetics for triphenylphosphine with the $Mn^{IV}(Me_2EBC)$ complexes in the absence/presence of Lewis acid. Conditions: solvent acetone, triphenylphosphine 40 mM, manganese(IV) complexes 2 mM, trifluoromethanesulfonate of redox-inactive metal ions 2 mM, 293K. Reprinted with permission from ref. 52. Copyright 2013 American Chemical Society.

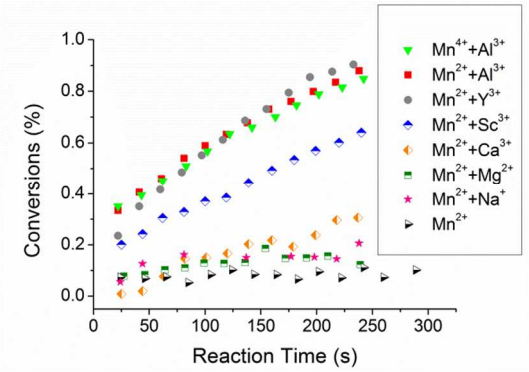

Fig. 6 Lewis acid accelerated oxygenation kinetics by the $Mn(Me_2EBC)Cl_2$ catalyst. Conditions: solvent acetone 5 mL, thioanisole 0.1 M, manganese(II) catalyst 0.33 mM, Lewis acid 0.33 mM, PhIO 0.6 mmol, 293 K, 4 h. Reprinted with permission from ref. 52. Copyright 2013 American Chemical Society.

As disclosed from $[(N4Py)Fe^{IV}(O)]^{2+}$ and $Mn^{IV}(Me_2EBC)(OH)^{2+}$ models, both Brönsted acid and Lewis acid can accelerate the redox metal ions mediated electron transfer rates, and obviously, the origins of their acceleration are similar. Acceleration by Brönsted acid originates from the protonation of the M^{n+}=O functional group, which leads to the positively shift of its potential. In the case of Lewis acid, acceleration originates from the formation of M^{n+}-O-LA^{m+} bridge or M^{n+}=O···LA^{m+} bond, which also lead to the similarly positive shift of its potential, and intrinsically, Fukuzumi and Nam proposed that it has also decreased the driving force of electron transfer ($\triangle G_{et}$).

Having extensively investigated the reactivity of the M^{n+}=O and its corresponding M^{n+}-OH moiety with $Mn^{IV}(Me_2EBC)(OH)_2(PF_6)_2$ model, Yin and co-workers summarized how the reactivity of an active metal ion in oxidation changes with its physicochemical properties such as metal-oxygen bond order, potential and net charge, etc. as follows:

1) with the positive net charge of a redox metal ion increasing, its redox potential would increase, and its electron transfer rate accelerates as well; however, its thermodynamic driving force in hydrogen abstraction may not change seriously due to the compensation effect between the potential and pK_a;
2) the distinct reactivity changes occur when the bond order of the metal-oxygen bond shifts from double to single bond (M^{n+}=O *vs* M^{n+}-OH): i) due to the protonation which leads to the increased net charge, the M^{n+}-OH has a higher redox potential than the corresponding M^{n+}=O, thus demonstrating more faster rate in electron transfer; ii) although they demonstrate similar capability in hydrogen abstraction because of the compensation effect, and have similar kinetic characters

in the transition state of hydrogen atom abstraction step, they demonstrate distinctly different reactivity after hydrogen abstraction. That is, after hydrogen abstraction, the reduced $M^{(n-1)+}$-OH from M^{n+}=O can rebind the OH group back to the substrate radical to generate hydroxylated product, whereas the $M^{(n-1)+}$-OH_2 from M^{n+}-OH cannot perform hydroxylation reaction; iii) in oxygenation, M^{n+}=O can concertedly transfer oxygen to substrate like olefin and phosphine, while oxygenation by the M^{n+}-OH proceeds through electron transfer, however, it does not oxygenate olefin.

4.2 The implications of the oxidative relationships of metal oxo and hydroxo moieties in oxidations

Disclosed reactivity differences between M^{n+}=O and M^{n+}-OH as summarized above have provided clues to understand the origins of the enzymes' choice on them. One major function of the P450s is to metabolize versatile robust organic molecules, for example, through hydroxylation. Thereof, the Fe^{IV}=O form of the functional group is essential to achieve this event by oxygen rebound mechanism, because, as disclosed above, a Fe^{IV}-OH functional group is incapable of achieving hydroxylation reaction (see Scheme 25 above). In another case, lipoxygenases need a Fe^{III}-OH or Mn^{III}-OH, rather than the corresponding Fe^{III}=O or Mn^{III}=O functional group to abstract hydrogen atom from unsaturated fatty acid for generating alkylperoxide products. If a Fe^{III}=O or Mn^{III}=O served hydrogen abstraction in lipoxygenase, further rebinding of the OH group back to the substrate radical may happen *in situ* as well as in P450s, which would block its dioxygen trapping to generate the targeted peroxide product (Scheme 28).[43] In chloroperoxidase, Green has identified its active intermediate compound II existing as Fe^{IV}-OH form,[7] while in other peroxidases, the form of compound II in Fe^{IV}=O or Fe^{IV}-OH form was even in arguments.[5, 53] These peroxidases, generally having a hydrophilic environment surrounding the active sites, are involved in electron transfer rather than oxygenation in nature. Therefore, their fruitful hydrogen-bonding networks around the active sites may facilitate the shift of the functional group of the compound II between Fe^{IV}=O or Fe^{IV}-OH as needed. Clearly, the different electron transfer ability of the M^{n+}=O and M^{n+}-OH as disclosed above has provided novel insights into the form of the compound II in those peroxidases.

The reactivity differences between M^{n+}=O and M^{n+}-OH also provide new clues to explain those elusive chemical oxidation phenomena. In heterogeneous oxidations with supported metal oxide catalysts, a popular phenomenon is that inputting ppm level of moisture would substantially accelerate the oxidation rate, for example, in CO oxidation, however, the roles of moisture are still in arguments until now. As a metal oxide catalyst, the dominant metal ion functional groups would be the terminal oxo (M^{n+}=O) or bridged oxo group (M^{n+}-O-M^{n+}), absorption of the moisture on the catalyst can protonate these functional groups to form M^{n+}-OH or M^{n+}-O(H)-M^{n+} group. Now, the disclosed distinct reactivity of M^{n+}=O and M^{n+}-OH in oxidations may provide new clues to rationalize the roles of moisture in those heterogeneous oxidation processes. Indeed, in investigating the low temperature CO oxidation, Zhang and others discovered that gold supported on metal hydroxides is more active than that supported on the corresponding oxides, and without the presence of gold, the ferrihydrite is much easier to reduce than crystalline Fe_2O_3, a process recalls that the M^{n+}-OH functional group can transfer electron faster than does the corresponding M^{n+}=O.[54]

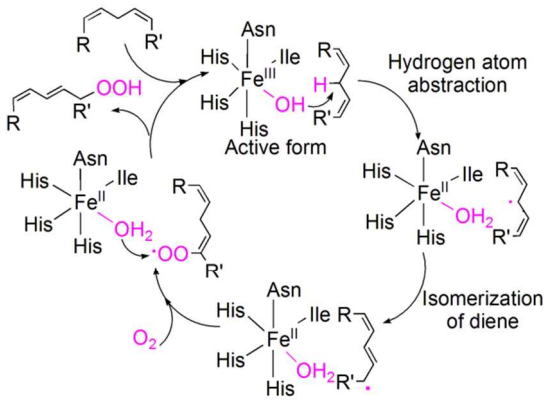

Scheme 28 Dioxygenation mechanism of the Fe^{III}-OH moiety in lipoxygenases (modified from ref. 34).

In redox catalyst design, the finding of increasing the positive net charge of an active species may enhance its redox potential has inspired Yin and co-workers to develop a non-redox metal ion promoted Pd(II)-catalyzed benzene hydroxylation (Scheme 29).[55] In ligand free Pd(II)-catalyzed C-H functionalization of benzene with dioxygen, it generally leads to the dominant formation of diphenyl through coupling, whereas the hydroxylation product, phenol, is always less produced. In the case of adding ligand, for example, 2,2-bipyridine (bpy), to generate steric hindrance for blocking the diphenyl formation, the ligated Pd(II) cation becomes incapable of functionalizing benzene due to its reduced oxidizing power. Similarly, 2,2'-bipyrimidine (bpym) also inactivates the Pd(II) cation in C-H bond functionalization of benzene. However, adding non-redox Al(III) to Pd^{II}(bpym) can regenerate the active Pd(II) species which is capable of selectively hydroxylzing benzene to phenol, and, significantly, formation of diphenyl was blocked due to the presence of the bpym ligand. Regenerating the oxidizing power of the Pd^{II}(bpym) by adding Al(III) has been attributed to the formation of the Al(III)-bpym-Pd(II) complex, which leads to the increases of the net charge of the Pd^{II}(bpym) intermediate, and positive shift of the redox potential of Pd^{2+}. Evidently, related isotope labelling experiments using benzene-d_6 revealed that adding Al(III) to Pd^{II}(bpym) causes abundant H/D exchange in both benzene substrate and phenol product, thus confirmed the promoted C-H bond activation capability of Pd^{II}(bpym) in the presence of Al(III). In another test, adding Al(III) to Pd^{II}(bpy) does not regenerate the catalytic activity of Pd(II), further confirming that recovery of the catalytic activity of Pd^{II}(bpym)

by adding Al(III) originates from the coordination of Al(III) to the Pd^{II}(bpym) complex through two distal nitrogen sites of bpym ligand, which positively shifts the potential of Pd(II), thereof improves its oxidizing ability.

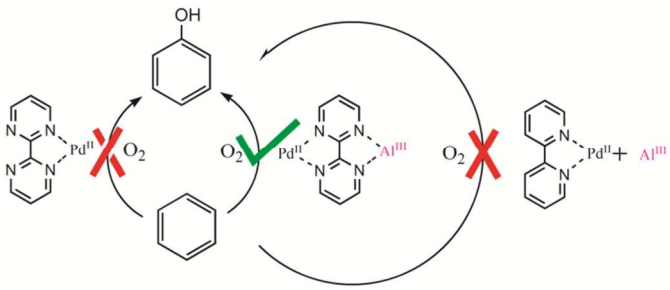

Scheme 29 Lewis acid promoted Pd(II)-catalyzed benzene hydroxylation (modified from ref.55).

5. Conclusions and perspective

As presented above, both redox M^{n+}=O and M^{n+}-OH moieties can play the crucial roles in a series of electron transfer, hydrogen atom transfer and oxygen transfer events, however, the redox enzymes' choices on them are not random, but highly specific. The available results from different models have gradually disclosed that they have distinct reactivity differences in oxidations in addition to their similarities, which provides new clues to understand their roles in a specific oxidation event. In particular, in the active site of redox enzymes, there commonly exists a fruitful network of hydrogen bond. With the formation and cleavage of hydrogen bond in the preceding of oxidation, the net charge in the reaction center may change simultaneously, and the active function group of the redox metal ion may have chance to shift between oxo and hydroxo form. The changes of these physicochemical properties in the active site of redox enzymes would apparently reflect the requirements of oxidation preceding. In addition, the identified X-ray structures of redox enzymes may not always reflect the real intermediate in a living oxidation step, which leads to misunderstandings and arguments from different labs about the active form of the redox enzymes. Understanding the oxidative relationships of active M^{n+}=O and M^{n+}-OH moieties can obviously help the elucidations of the enzymatic mechanisms, thus benefit the rationalization of the active form of the metal ion which is not feasibly identified *in situ* in a catalytic cycle.

Clearly, well-understanding of the reactivity relationships of the M^{n+}=O and M^{n+}-OH moieties may also help the explanations of those elusive oxidative phenomena like the roles of moisture in heterogeneous oxidations, thus benefit the design of selective redox catalysts. As stated earlier, the viable difference between M^{n+}=O and M^{n+}-OH moiety is the different protonation state of the metal ion, which leads to their significant reactivity differences. Although the protonation is a behaviour of Brönsted acid, Lewis acid can share the similar roles of Brönsted acid to the significant extent, that is, M^{n+}-OH *vs* M^{n+}-O-LA^{m+} or M^{n+}=O···LA^{m+} (LA: Lewis acid), and the available data do confirm their similarities (*via supra*). Thereof, the oxidative relationships of M^{n+}=O and M^{n+}-OH discussed in this review may also help understanding the roles of those non-redox metal ions in versatile biological and chemical oxidations. The well-known examples include adding redox inactive metal ions as additives to metal oxide catalysts for modifying their reactivity and stability, and even in a pure metal oxide catalyst, the second metal ion in M^{n+}-O-M^{n+} bridge may also function as a Lewis acid. At the end of this review, it is worth to mention that the influences of the non-redox metal ions as Lewis acid on the active M^{n+}=O moieties have attracted much attention recently. Through comparing how Brönsted acid and Lewis acid affect the reactivity of the redox metal ions would obviously benefit the comprehensively understanding of these oxidation events in biological and chemical communities.

Acknowledgements

The funds from NSFC (No 21303063 and 21273086) and the Project of Chutian Scholar foundation, Hubei province are deeply appreciated. Yin is also grateful for the co-workers and the technician staffs in the Analytical and Testing Center of Huazhong University of Science and Technology.

Notes and references

Key Laboratory for Large-Format Battery Materials and System, Ministry of Education, School of Chemistry and Chemical Engineering, Huazhong University of Science and Technology, Wuhan 430074, PR China, Fax: 86-27-87543632; Tel: 86-27-87543732; E-mail: gyin@hust.edu.cn.

1. S. Fukuzumi, *Coord. Chem. Rev.*, 2013, **257**, 1564.
2. J. J. Warren, T. A. Tronic and J. M. Mayer, *Chem. Rev.*, 2010, **110**, 6961.
3. B. Meunier and J. Bernadou, *Metal-Oxo and Metal-Peroxo Species in Catalytic Oxidations*, 2000, **97**, 1.
4. E. I. Solomon, J. Zhou, F. Neese and E. G. Pavel, *Chem. Biol.*, 1997, **4**, 795.
5. H. P. Hersleth, U. Ryde, P. Rydberg, C. H. Gorbitz and K. K. Andersson, *J. Inorg. Biochem.*, 2006, **100**, 460.
6. J. T. Groves, *Journal of Chemical Education*, 1985, **62**, 928.
7. M. T. Green, J. H. Dawson and H. B. Gray, *Science*, 2004, **304**, 1653.
8. J. F. Hull, D. Balcells, E. L. O. Sauer, C. Raynaud, G. W. Brudvig, R. H. Crabtree and O. Eisenstein, *J. Am. Chem. Soc.*, 2010, **132**, 7605.
9. W. Liu, X. Y. Huang, M. J. Cheng, R. J. Nielsen, W. A. Goddard and J. T. Groves, *Science*, 2012, **337**, 1322.
10. S. B. Karki, J. P. Dinnocenzo, J. P. Jones and K. R. Korzekwa, *J. Am. Chem. Soc.*, 1995, **117**, 3657.
11. R. E. P. Chandrasena, K. P. Vatsis, M. J. Coon, P. F. Hollenberg and M. Newcomb, *J. Am. Chem. Soc.*, 2004, **126**, 115.
12. H. Hirao, D. Kumar, L. Que and S. Shaik, *J. Am. Chem. Soc.*, 2006, **128**, 8590.
13. A. S. Larsen, K. Wang, M. A. Lockwood, G. L. Rice, T. J. Won, S. Lovell, M. Sadilek, F. Turecek and J. M. Mayer, *J. Am. Chem. Soc.*, 2002, **124**, 10112.
14. S. Fukuzumi, N. Fujioka, H. Kotani, K. Ohkubo, Y. M. Lee and W. Nam, *J. Am. Chem. Soc.*, 2009, **131**, 17127.
15. J. T. Groves, J. B. Lee and S. S. Marla, *J. Am. Chem. Soc.*, 1997, **119**, 6269.

16. G. Jiang, J. Chen, H. Y. Thu, J. S. Huang, N. Zhu and C. M. Che, *Angew. Chem. Int. Edit.*, 2008, **47**, 6638.
17. J. P. Caradonna, P. R. Reddy and R. H. Holm, *J. Am. Chem. Soc.*, 1988, **110**, 2139.
18. S. Kundu, J. V. Thompson, A. D. Ryabov and T. J. Collin, *J. Am. Chem. Soc.*, 2011, **133**, 18546.
19. A. Corma, I. Dominguez, A. Domenech, V. Fornes, C. J. Gomez-Garcia, T. Rodenas and M. J. Sabater, *J. Catal.*, 2009, **265**, 238.
20. R. L. Osborne, M. K. Coggins, J. Terner and J. H. Dawson, *J. Am. Chem. Soc.*, 2007, **129**, 14838.
21. A. Brausam, S. Eigler, N. Jux and R. van Eldik, *Inorg. Chem.*, 2009, **48**, 7667.
22. H. Yoon, Y. Morimoto, Y. M. Lee, W. Nam and S. Fukuzumi, *Chem. Commun.*, 2012, **48**, 11187.
23. B. Chiavarino, R. Cipollini, M. E. Crestoni, S. Fornarini, F. Lanucara and A. Lapi, *J. Am. Chem. Soc.*, 2008, **130**, 3208.
24. K. Nehru, M. S. Seo, J. Kim and W. Nam, *Inorg. Chem.*, 2007, **46**, 293.
25. T. H. Parsell, M. Y. Yang and A. S. Borovik, *J. Am. Chem. Soc.*, 2009, **131**, 2762.
26. O. Pestovsky and A. Bakac, *J. Am. Chem. Soc.*, 2003, **125**, 14714.
27. N. Mizuno and K. Kamata, *Coord. Chem. Rev.*, 2011, **255**, 2358.
28. A. M. Khenkin, G. Leitus and R. Neumann, *J. Am. Chem. Soc.*, 2010, **132**, 11446.
29. J. H. Lan, Z. Q. Chen, J. C. Lin and G. C. Yin, *Green Chem.*, 2014, **16**, 4351.
30. M. Hamberg, C. Su and E. Oliw, *J. Biol. Chem.*, 1998, **273**, 13080.
31. S. Ogo, R. Yamahara, M. Roach, T. Suenobu, M. Aki, T. Ogura, T. Kitagawa, H. Masuda, S. Fukuzumi and Y. Watanabe, *Inorg. Chem.*, 2002, **41**, 5513.
32. A. L. Stockert, S. S. Shinde, R. F. Anderson and R. Hille, *J. Am. Chem. Soc.*, 2002, **124**, 14554.
33. C. R. Goldsmith and T. D. P. Stack, *Inorg. Chem.*, 2006, **45**, 6048.
34. C. R. Goldsmith, A. P. Cole and T. D. P. Stack, *J. Am. Chem. Soc.*, 2005, **127**, 9904.
35. G. C. Yin, J. M. McCormick, M. Buchalova, A. M. Danby, K. Rodgers, V. W. Day, K. Smith, C. M. Perkins, D. Kitko, J. D. Carter, W. M. Scheper and D. H. Busch, *Inorg. Chem.*, 2006, **45**, 8052.
36. I. Garcia-Bosch, A. Company, C. W. Cady, S. Styring, W. R. Browne, X. Ribas and M. Costas, *Angew. Chem. Int. Edit.*, 2011, **50**, 5647.
37. P. J. Donoghue, J. Tehranchi, C. J. Cramer, R. Sarangi, E. I. Solomon and W. B. Tolman, *J. Am. Chem. Soc.*, 2011, **133**, 17602.
38. G. C. Yin, A. M. Danby, D. Kitko, J. D. Carter, W. M. Scheper and D. H. Busch, *J. Am. Chem. Soc.*, 2007, **129**, 1512.
39. G. C. Yin, A. M. Danby, D. Kitko, J. D. Carter, W. M. Scheper and D. H. Busch, *J. Am. Chem. Soc.*, 2008, **130**, 16245.
40. T. Kurahashi, A. Kikuchi, T. Tosha, Y. Shiro, T. Kitagawa and H. Fujii, *Inorg. Chem.*, 2008, **47**, 1674.
41. A. T. Fiedler and L. Que, *Inorg. Chem.*, 2009, **48**, 11038.
42. Y. J. Wang, S. Shi, H. J. Wang, D. J. Zhu and G. C. Yin, *Chem. Commun.*, 2012, **48**, 7832.
43. S. Shi, Y. J. Wang, A. H. Xu, H. J. Wang, D. J. Zhu, S. B. Roy, T. A. Jackson, D. H. Busch and G. C. Yin, *Angew. Chem. Int. Edit.*, 2011, **50**, 7321.
44. A. H. Xu, H. Xiong and G. C. Yin, *Chem.-Eur. J.*, 2009, **15**, 11478.
45. Y. J. Wang, J. Y. Sheng, S. Shi, D. J. Zhu and G. C. Yin, *J. Phys. Chem. C*, 2012, **116**, 13231.
46. M. K. Coggins, L. M. Brines and J. A. Kovacs, *Inorg. Chem.*, 2013, **52**, 12383.
47. D. E. Lansky and D. P. Goldberg, *Inorg. Chem.*, 2006, **45**, 5119.
48. C. E. MacBeth, R. Gupta, K. R. Mitchell-Koch, V. G. Young, G. H. Lushington, W. H. Thompson, M. P. Hendrich and A. S. Borovik, *J. Am. Chem. Soc.*, 2004, **126**, 2556.
49. J. Park, Y. Morimoto, Y. M. Lee, W. Nam and S. Fukuzumi, *J. Am. Chem. Soc.*, 2012, **134**, 3903.
50. Y. Morimoto, H. Kotani, J. Park, Y. M. Lee, W. Nam and S. Fukuzumri, *J. Am. Chem. Soc.*, 2011, **133**, 403.
51. J. Park, Y. Morimoto, Y. M. Lee, W. Nam and S. Fukuzumi, *J. Am. Chem. Soc.*, 2011, **133**, 5236.
52. L. Dong, Y. J. Wang, Y. Z. Lv, Z. Q. Chen, F. M. Mei, H. Xiong and G. C. Yin, *Inorg. Chem.*, 2013, **52**, 5418.
53. R. K. Behan and M. T. Green, *J. Inorg. Biochem.*, 2006, **100**, 448.
54. L. Li, A. Q. Wang, B. T. Qiao, J. Lin, Y. Q. Huang, X. D. Wang and T. Zhang, *J. Catal.*, 2013, **299**, 90.
55. H. J. Guo, Z. Q. Chen, F. M. Mei, D. J. Zhu, H. Xiong and G. C. Yin, *Chem-Asian J.*, 2013, **8**, 888.

